HHS Public Access

Author manuscript

Sci Immunol. Author manuscript; available in PMC 2020 December 12.

Published in final edited form as:

Sci Immunol. 2020 June 12; 5(48): . doi:10.1126/sciimmunol.aba6087.

Single-cell transcriptomic analysis of allergen-specific T cells in allergy and asthma

Grégory Seumois[1,†,*], **Ciro Ramírez-Suástegui**[1,†], **Benjamin J. Schmiedel**[1], **Shu Liang**[1], **Bjoern Peters**[1,3], **Alessandro Sette**[1,3], **Pandurangan Vijayanand**[1,2,3,*]

[1]La Jolla Institute for Allergy and Immunology, La Jolla, CA 92037, United States

[2]Clinical and Experimental Sciences, National Institute for Health Research Southampton Respiratory Biomedical Research Unit, University of Southampton, Faculty of Medicine, Southampton SO166YD, United Kingdom

[3]Department of Medicine, University of California San Diego, La Jolla, CA 92037, United States

Abstract

CD4$^+$ helper T cells (T_H) and regulatory T cells (T_{reg}) that respond to common allergens play an important role in driving and dampening airway inflammation in patients with asthma. Until recently, direct, unbiased molecular analysis of allergen-reactive T_H and T_{reg} cells has not been possible. To better understand the diversity of these T cell subsets in allergy and asthma, we analyzed the single-cell transcriptome of ~50,000 house dust mite (HDM) allergen-reactive T_H cells and T_{reg} cells from asthmatics with HDM allergy and from three control groups: asthmatics without HDM allergy and non-asthmatics with and without HDM allergy. Our analyses show that HDM allergen-reactive T_H and T_{reg} cells are highly heterogeneous, and certain subsets are quantitatively and qualitatively different in subjects with HDM-reactive asthma. The number of interleukin (IL)-9 expressing HDM-reactive T_H cells is greater in asthmatics with HDM allergy compared to non-asthmatics with HDM allergy, and this IL-9-expressing T_H subset displays enhanced pathogenic properties. More HDM-reactive T_H and T_{reg} cells expressing the interferon-response signature (T_HIFNR and T_{reg}IFNR) are present in asthmatics without HDM allergy compared with those with HDM allergy. In cells from these subsets (T_HIFNR and T_{reg}IFNR), expression of *TNFSF10* was enriched; its product, tumor necrosis factor-related apoptosis-inducing ligand (TRAIL), dampens activation of T_H cells. These findings suggest that the T_HIFNR and T_{reg}IFNR subsets may dampen allergic responses, which may help explain why only some people develop T_H2 responses to nearly ubiquitous allergens.

[*]Correspondence should be addressed to P.V. (vijay@lji.org) or G.S. (gregory@lji.org).

[†]These authors contributed equally to this work

Author contributions: G.S, A.S, B.P, and P.V. conceived of the work; G.S, C.R-S, P.V designed and analyzed the experiments and single-cell RNA seq data and wrote the paper; B.S. performed FACS and ARTE assays as well as TRAIL culture assays. G.S. and S.L performed bulk and single-cell RNA-seq experiments; and all authors read and approved the final text of the manuscript.

Competing interests: P.V received research funding unrelated to this work from Pfizer. G.S. received a career development fellowship award from Kyowa Kirin Pharmaceutical Research Inc. to independently pursue research on IL-9 in severe asthma. P.V. and G.S. are listed as inventors on a provisional patent application covering findings reported in this manuscript. The other authors declare that they have no competing interests.

Data availability: Scripts are available in our repository on GitHub (https://github.com/vijaybioinfo/hdm_2019). Sequencing data for this study has been deposited into the Gene Expression Omnibus under GSE146172. including GSE146046 for bulk-RNA-seq and GSE146170 for single-cell datasets.

One sentence summary

Single-cell transcriptomic analysis of allergen-specific T cells in allergy and asthma reveals new T cell subsets.

Introduction

Asthma is characterized by aberrant type 2 immune responses to common inhaled aeroallergens such as house dust mite (HDM), grass pollen, animal dander, and mold (1–6), leading to 'asthma attacks' in sensitized asthmatic subjects in response to inhalation of such allergens (7). The hallmarks of asthma, namely airway narrowing and sputum eosinophilia, have been shown to result from the specific activation of (MHC) class II–restricted $CD4^+$ helper T cells (T_H) by challenging asthmatics with synthetic allergen-derived peptides (8–12). Further evidence of the centrality of T_H cells in asthma pathology is that their depletion reduces allergic airway inflammation in animal models (13), and that inhibition of T_H cell-derived type 2 cytokines (IL-5, IL-13, IL-4) is clinically beneficial in patients with asthma (14–17). However, despite the central role of allergen-reactive T_H cells and their products in driving airway inflammation, the full spectrum and function of T_H cell subsets that respond to common allergens has yet to be defined. Similarly, though an imbalance between regulatory T cells (T_{reg}) and T_H cell responses to allergens is associated with the development of allergy and asthma (18–23), the heterogeneity of allergen-reactive T_{reg} cells remains unstudied.

Previous studies of allergen-reactive T cells have characterized their phenotype based on the expression of cell-surface markers or canonical cytokines (24–26). Due to their relative rarity, analyses of these cells usually require *in vitro* expansion, which can alter their molecular properties, thus limiting the value of unbiased transcriptomic studies (27–29). Furthermore, transcriptomic studies performed at the whole population level fail to capture cellular heterogeneity and also lack the resolution to detect biological differences associated with asthma or allergy (30). A recent single-cell analysis of T_H cells in a mouse models of allergic airway inflammation revealed substantial heterogeneity, and also identified T_H subsets that had not been previously described (20).

Characterizing the various subsets of T_H and T_{reg} cells in asthmatic subjects and comparing their frequency and properties to those in subjects without asthma is ideally achieved at single-cell resolution. Indeed, single-cell transcriptomic analysis can help define the molecular properties of allergen-reactive T_H cells associated with pathology and assess whether these features are the result of an expansion of a pre-existing population of cells or the result of their aberrant differentiation in response to environmental signals (31, 32). To address the latter issue, the subsets of allergen-reactive T_H cells must also be defined in subjects without asthma and allergy. Such allergen-reactive T_H cells are present even in non-allergic subjects (33–36), although it is not known why or how these cells fail to cause overt allergic responses.

To address these questions in a hypothesis-free manner, we performed single-cell transcriptomic analysis of T_H and T_{reg} cells that react to house dust mite allergen (HDM).

HDM is one of the most common and ubiquitous allergens, and sensitization is associated with both the onset of allergic asthma and its severity (37–40). The relatively high abundance of HDM-reactive T cells in the blood makes it is possible to isolate sufficient number of cells for high-throughput single-cell transcriptomic analysis. Here, we report on the single-cell transcriptomes of >50,000 HDM-reactive T cells from allergic asthmatic subjects and relevant control groups. Our analysis revealed multiple distinct subsets of T_H and T_{reg} cells that are either preferentially expanded or depleted in asthmatic subjects with and without HDM allergy, defined the pathogenic properties of T_H subsets associated with allergic asthma, and uncovered a unique HDM-reactive T_H subset that is expanded specifically in subjects without HDM allergy.

Results

Bulk RNA-seq analysis of HDM allergen-reactive T cells does not identify asthma-specific features

To comprehensively characterize the molecular properties of allergen-reactive T_H and T_{reg} cells from patients with asthma, we isolated pure populations of HDM-reactive memory T_H and T_{reg} cells *ex vivo* (see Materials and Methods and fig. S1) from asthmatics with HDM allergy (N = 6) and performed both bulk and single-cell RNA-seq (Fig. 1A). To distinguish the molecular features that are specific to asthma as opposed to HDM allergy, we performed similar assays in HDM-reactive T_H and T_{reg} cells isolated from HDM-allergic subjects without asthma (N = 6). Because allergen-reactive T cells are present even in non-allergic subjects (33–36), we also isolated HDM-reactive T_H and T_{reg} cells from asthmatic (N = 6) and healthy subjects (N = 6) without HDM allergy to uncover features that may contribute to the lack of HDM allergy i.e., IgE reactivity. In total, we performed 95 bulk RNA-seq and ~50,000 single-cell RNA-seq assays on T cells from a total of 24 subjects (Fig. 1A, and table S1).

HDM-reactive T_H cells (0.2–3 % of all memory T_H cells) and T_{reg} cells (1–5 % of all memory T_{reg} cells) were detected in all 4 subject groups, including the HDM-allergic and non-allergic subjects (Fig. 1B). Bulk transcriptome analysis showed that HDM-reactive T_H and T_{reg} cells clustered separately from one another and from HDM-non-reactive cells (HDM^- T cells) (Fig. 1C). 724 transcripts were differentially expressed between both HDM-reactive, activated T cells populations, T_H and T_{reg} (following stimulation with HDM peptide/MHC complex from antigen-presenting cells) and HDM^- T cells (not stimulated by HDM-allergen derived peptides) (adjusted P-value < 0.01, $\log_2$ fold change > 2, Fig. 1D and table S2). As expected, these differentially expressed transcripts were highly enriched for genes in the TCR signaling pathway (Fig. 1E, top panel). Allergen-activated HDM-reactive T_H cells expressed greater amounts of several transcripts encoding cytokines (*IL-2, −13, −5, -4, −9, −31 −17F, −22, TNF, IFNG, CSF-2*) and chemokines (*CCL20, CXCL10*) linked to effector functions (Fig. 1E, middle panel). HDM-reactive T_{reg} cells expressed higher levels of genes linked to T_{reg} function, such as *IL2RA*, *FOXP3*, *CTLA4*, *IKZF2*, *TNFRSF8*, when compared with HDM^- T cells (Fig. 1E, bottom panel, fig. S2, and table S2).

Clustering analysis of HDM-reactive T_H cells by disease group showed separation based on HDM allergy status rather than asthma phenotype (Fig. 1F). For example, in HDM-reactive

T_H cells from HDM-allergic subjects, expression of canonical T_H2 cytokines was increased compared with those from HDM-non-allergic subjects (Fig. 1G), whereas no significant differences were observed between the HDM-reactive T_H cells from asthmatic versus non-asthmatic subjects with HDM allergy (Fig. 1G). The heterogeneity observed within the HDM-reactive T_H population, reflected in the co-expression of transcripts encoding canonical T_H1, T_H2 and T_H17 cytokines (Fig. 1H), is likely to have limited the resolution of bulk transcriptome data to distinguish asthma-specific features.

Single-cell RNA-seq analysis reveals heterogeneity among HDM-reactive T_H cells

Single cells from all 6 subjects in each disease group were pooled for droplet-based single-cell RNA-seq (10x Genomics platform), and genotype-based deconvolution was employed to obtain subject-specific single-cell transcriptomes and to exclude potential cell doublets (see Materials and Methods, and fig. S3). Our cell isolation strategy, based on the CD154 activation marker, primarily enriches for HDM-reactive T_H cells (41–43). Analogous to flow cytometry-based approaches, single-cell transcriptome analysis allows discrimination of activated (true positives) from non-activated (false positives) T_H cells. Based on a T_H activation signature, derived by comparing HDM-reactive T_H and HDM-non-reactive (HDM^- T cells) single cells (Fig. 2A and fig. S3), we eliminated potential false positive cells from the HDM-reactive T_H cell population (Fig. 2A and fig. S3).

Analysis of the single-cell transcriptomes of HDM-reactive T_H cells (non-doublet and activation-signature positive) revealed 7 clusters (Materials and Methods, and fig. S4) present at varying frequency among subjects, highlighting the importance of studying cells from multiple subjects (Fig. 2B and fig. S5). To understand the molecular properties unique to each cluster, we performed multiple pair-wise single-cell differential gene expression analyses (Materials and Methods, and table S3). Several hundred genes (N = 687) were especially highly expressed by each cluster, allowing classification into specific T_H subsets (Fig. 2C). Cells in cluster 1 were highly enriched for transcripts encoding canonical type 2 cytokine genes (*IL5*, *IL13*, *IL4*), the T_H2 master transcription factor *GATA3*, and receptors (*IL1RL1* and *IL17RB*) for the T_H2-polarizing cytokines IL-33 and IL-25, indicating that this cluster represented T_H2 cells (Fig. 2D). Notably, the T_H2 subset only represented ~6.3 % of the HDM-reactive T_H cell population (Fig. 2B). Cluster 2 was enriched for T_H1 phenotype- and function-related genes such as *IFNG, CXCR3*, and *PRF1* (44–47) (Fig. 2, C and D). In addition, we found that the expression of genes encoding the chemokines XCL1 and XCL2 was correlating with expression of *IFNG* (fig. S6), suggesting a potentially important role of these chemokines in the function of T_H1 cells (46–49). Cluster 3 was enriched for T_H17 phenotype- and function-related genes such as *IL17A, IL17F, CCR6, IL22, CTSH,* and *CCL20* (50–52). The characteristics of cell clusters 1–3 were confirmed by gene set enrichment analysis (GSEA) using curated lists of signature genes (Fig. 2E and table S4). Cells in cluster 4 were very highly enriched for type I and II interferon response genes (*IFI6, MX1, ISG20, OAS1, IFIT1, IFI44L*) (53, 54), indicating that they represent a previously uncharacterized T_H subset, which we termed T_H subset expressing the interferon response signature (T_HIFNR) (Fig. 2, C and D). GSEA analysis confirmed enrichment of interferon response genes in this cluster (Fig. 2E and table S4). Cells in clusters 5, 6, and 7 were enriched for genes linked with cell activation; cluster 5 (T_HACT1) was enriched in genes

linked to ribosomal proteins and RNA translation (*RPL*x, *RPS*x, see table S3), cluster 6 (T_HACT2) was enriched with genes linked to endocytosis and membrane trafficking (*ARL6IP5*, *ARPC5*, *BIN1,* see table S3), and cluster 7 (T_HACT3) was enriched in genes linked to chromosome maintenance (*NPM1*, *NHP2*) and apoptosis (*GADD45B*, *NFKB1*, *ATF4*, *PMAIP1,* see table S3). Overall, our single-cell transcriptome analysis uncovered substantial heterogeneity among HDM-reactive T_H cells.

Proportions of HDM-reactive T_H subsets differ between HDM allergic and non-allergic subjects

We next asked if the proportions of any of the HDM-reactive subsets varied between subjects with or without HDM allergy or asthma. As expected, the T_H2 cluster (cluster 1) was present only in the HDM-allergic groups (Fig. 3, A and B, and fig. S7), consistent with the central role of T_H2 cells and type 2 cytokines in IgE class switching and allergy and asthma pathogenesis (55–57). On the other hand, the T_H1 cluster, though observed in all subject groups, was present at greater proportions in subjects without HDM allergy, consistent with the reciprocal role of T_H1 cells in dampening T_H2 differentiation. Several other clusters, including the T_H17 cluster, showed no significant differences in their proportions among disease and control groups (Fig. 3, A and B, and fig. S7).

Subjects without HDM allergy – both the asthmatic and healthy control groups – despite displaying a substantially broad T_H response to HDM allergen, failed to generate T_H2 cells that respond to HDM *ex vivo*. Strikingly, the large majority of HDM-reactive T_H cells expressing the interferon response signature (T_HIFNR, cluster 4) were observed in subjects without HDM allergy (Fig. 3, A, B and C). This negative association raised the possibility that the T_HIFNR subset plays a role in dampening T_H2 responses to allergens. Intriguingly, cells in the T_HIFNR subset expressed the highest levels of *CXCL10* and *TNFSF10* (Fig. 3D). *CXCL10* encodes CXCL10, a chemokine that recruits T_H cells expressing the chemokine receptor CXCR3, which mainly comprises T_H1 cells (58, 59). Thus, *CXCL10* expression by T_HIFNR cells is likely to promote selective recruitment of T_H1 cells (60). *TNFSF10* encodes tumor necrosis factor-related apoptosis-inducing ligand (TRAIL), which can drive apoptosis in cells expressing its receptors (TRAIL-R) (61, 62). More recently, both surface-bound and soluble TRAIL have been shown to dampen TCR signaling by inhibiting the phosphorylation of downstream kinases (63–66). Given that activated T_H cells express TRAIL-R (65, 66), TRAIL produced by the HDM-reactive T_HIFNR cells may play an important role in blocking T_H cell responses to HDM *in vivo*. Interestingly, a small fraction of cells expressing T_HIFNR signature genes (*IFI6*, *ISG15*) and *TNFSF10* were observed even in resting cells not reactive to HDM, suggesting persistence of this population within PBMC (Fig. 3E). We confirmed that following TCR stimulation TRAIL was expressed by population of T_H cells, which is likely to be enriched for the T_HIFNR subset (Fig. 3F). In published single-cell datasets (67) we found $CD4^+$ T cells in human lungs expressed interferon-response signature genes and *TRAIL*, which indicated that the T_HIFNR subset is also present in the human lung tissue (fig. S8). We next experimentally tested TRAIL's function and found that recombinant TRAIL inhibited TCR-dependent activation of T_H cells *ex vivo*, as measured by the surface expression of the activation markers CD154, CD69, and

CD137 (4–1BB) (68) (Fig. 3, G and H). These findings support a potential regulatory role of HDM-reactive T_HIFNR cells in dampening allergic responses.

A subset of HDM-reactive T_{reg} cells express the interferon response signature

We also investigated whether HDM-reactive T_{reg} cells differed between HDM allergic and non-allergic subjects. As shown previously, we confirmed that the proportion of HDM-reactive T_{reg} cells was not related to HDM allergic status (Fig. 1B) (43). Furthermore, transcriptomic analysis of bulk populations of HDM-reactive T_{reg} cells revealed no major disease-related differences (fig. S9). To determine whether specific subsets of HDM-reactive T_{reg} cells varied with disease state, we performed single-cell transcriptomic analysis of ~10,000 HDM-reactive T_{reg} cells across the 4 subject groups, which separated this population into 3 distinct clusters (Fig. 4, A and B, and table S3). The proportion of cells in cluster 2 was greater in asthmatic subjects without HDM allergy compared with HDM-allergic asthmatics, suggesting preferential expansion of this subset in asthmatic subjects without HDM allergy (Fig. 4, C and D, and fig. S10). GSEA analysis of transcripts enriched in this cluster (N = 248) revealed significant enrichment of interferon response genes (Fig. 4E). The features of this T_{reg} cluster were similar to those of the T_HIFNR cluster, which was also present at higher proportions in subjects without HDM allergy; for example, interferon-responsive T_{reg} cells (T_{reg}IFNR) also expressed higher levels of transcripts encoding for TRAIL (Fig. 4F). Overall, our findings indicate preferential expansion of HDM-reactive T_{reg} and T_H cells expressing the interferon response signature in asthmatic subjects without HDM allergy, and that expression of TRAIL by these subsets is likely to play an important role in dampening T_H2 responses to HDM allergens, although further studies in animal models would be required to confirm this hypothesis.

HDM-reactive T_H2 cells are enriched for transcripts linked to enhanced functionality

Given the important role of T_H2 cells in the pathogenesis of allergy and asthma, we analyzed the genes enriched in the T_H2 cluster to gain insights into their functional properties. Gene co-expression analysis is a powerful method to discover new genes that are likely to play important role in the differentiation or function of a given cell type (69, 70). Hierarchical gene clustering (Fig. 3A) and weighted gene co-expression network analysis (WGCNA) (71) (Materials and Methods, and Fig. 3B) of the 214 'T_H2 enriched' transcripts, defined from single-cell transcriptome analysis (Fig. 2, A and B), revealed 5 modules of highly co-expressed genes (Fig. 5A). Among these 5 modules, 2 modules (green and purple) contained genes linked to cellular metabolism, protein trafficking, active transcription and oxidative phosphorylation (*EIF3J*, *EIF5B*, *CALM3*, *FKBP1A*, *PTPN11*, *ATP13A3*, *PSMD13*, *UBE2S*, *DUSP4*), indicating increased metabolic and transcriptional activity in T_H2 cells; a third (blue) module contained genes encoding for important transcription factors linked to T_H2 cell differentiation such as GATA3, IRF4, and SATB1 (72–74).

The module including the canonical type 2 cytokine genes (*IL5*, *IL13*) (red in Fig. 5, A and B), likely includes other genes that play an important role in driving the effector functions of T_H2 cells. One of the most highly co-expressed transcripts encodes for the effector cytokine IL-9, which has recently been shown to be produced by a subset of T_H2 cells that expressed PPAR-γ following TGF-β signaling (75). We found that transcripts encoding for PPAR-γ

and the TGF-β receptor 3 (*TGFBR3*) were also enriched in T_H2 cells and highly co-expressed with *IL9* (Fig. 5, A and B), suggesting that the IL-9 differentiation pathway is active in T_H2 cells. Finally, transcripts linked to cytotoxicity function (*GZMB*, *RAB27A* (76–78)) and differentiation of cytotoxic T_H cells (*ZEB2*, *RUNX*3 (46, 77, 79)) were also highly co-expressed with *IL5* and *IL13*, indicating that HDM-reactive cells may include cytotoxic T_H2 cells (Fig. 5, A and B). Cytotoxic T_H cells are known to contribute to antiviral immunity (77, 80) and autoimmunity (81), and our findings bring up the possibility that they may also play a role in asthma pathogenesis.

The gene for another canonical type 2 cytokine, IL-4, also linked to the function of T follicular helper cells (T_{FH}) and IgE class switching, was present in a fourth module (yellow). Important molecules encoded by genes in this module include IL-31, a member of the IL-6 family of cytokines that is produced by activated T_H2 cells and leads to itching in skin inflammation (Fig. 5, A and B) (82, 83), and IL-3, which is linked to hematopoietic progenitor proliferation and recruitment (84–86). We recently showed that IL-3 plays an important role in the activation and survival of eosinophils (87). Other genes in this module encode for products such as ICOS and IL-21, which is linked to B cell help and immunoglobulin isotype class switching (Fig. 5, A and B), suggesting that this module was enriched for genes linked to T_{FH} cell function. The presence of gene modules with distinct co-expression patterns indicated potential heterogeneity in the T_H2 population. To address this issue, we re-clustered cells only from the T_H2 population; this analysis revealed 2 distinct sub-clusters (Fig. 5C), each highly enriched for genes in modules 3 and 4 (yellow and red) (Fig. 5, D, E and F).

Overall, these results show that cells in the T_H2 cluster were enriched for the expression of transcripts encoding for several co-stimulatory and inhibitory receptors as well as transcription factors and molecules known to promote T cell survival. The expression of the first class of molecules, including CD28, ICOS, BTLA, CTLA-4, PD-1, HVEM receptor (LIGHT, TNFSF14) (88), suggests that these molecules could be targeted to dampen the pro-inflammatory function of T_H2 cells in asthma. Pro-survival factors included several in the NF-κB signaling pathway, including NFKBID, NIPAI, MAP3K8, FOSL2, NEDD9 (89), ZEB2, BCL2A1 (90), BIRC3 (91), DUSP4/MKP-2 (92, 93), CFLAR (cFLIP/CASPER) (94). Together, these expression patterns suggest that these cells are endowed with properties that allow them to exert sustained and strong type 2 inflammatory responses in asthma.

IL-9-expressing HDM-reactive T_H2 cells are increased in asthma

We next sought to identify potential asthma-specific changes in HDM-reactive T_H2 cells from subjects with HDM allergy. Single-cell differential gene expression analysis of HDM-reactive T_H2 cells from HDM-allergic asthmatics versus non-asthmatics revealed that among the T_H2-enriched transcripts, *IL9* was the most upregulated gene in asthmatic subjects (Fig. 6A). Furthermore, as shown in Figure 5, D and E, sub-clustering of the T_H2 subset showed that *IL9*-expressing cells were highly enriched in the larger T_H2 sub-cluster (Fig. 6B). The relative proportion of cells in the *IL9*-enriched T_H2 subset (T_H2-cluster 1) was greater in asthmatics compared with (75) non-asthmatic subjects (Fig. 6C). Thus, enrichment of *IL9* expression in T_H2 cells appears to be associated in the development of asthma.

To determine the properties of *IL9*-expressing HDM-reactive T_H2 cells in asthmatic subjects, we compared the single-cell gene expression profiles of *IL9*-expressing and non-expressing cells contained within the *IL9*-enriched T_H2-cluster 1. We were surprised to find that expression of several transcripts encoding products linked to pathogenicity and survival of T_H2 cells was increased in *IL9*-expressing cells (Fig. 6D and table S3). These included transcripts encoding canonical T_H2 cytokine IL-5, cytotoxicity molecules (granzyme B, ZEB2, EFHD2), T_H2 polarizing and survival-related signaling receptor (IL-33R) (95, 96), and CD109, a membrane-anchored molecule described as negative regulator of TGF-β signaling (97, 98) but also as a co-activator of the JAK/STAT3 signaling pathway (98–100) that is important for T_H2 cell development (98, 101) (Fig. 6D, fig. S11, and table S3). Overall, these findings suggest that *IL9*-expressing HDM-reactive T_H2 cells displayed greater pathogenic properties that could play an important role in driving asthma pathogenesis.

Discussion

In this study, we present large-scale single-cell transcriptome analysis of allergen-reactive T_H and T_{reg} cells (N ~ 50,000) from subjects with asthma and/or allergy and healthy controls. Our characterization of HDM-reactive T_H cells identified substantial heterogeneity as well as quantitative and qualitative changes related to allergy and asthma and revealed a unique subset of T_H cells with a strong interferon response signature.

Our single-cell study addresses some of the important unanswered questions in the field of allergy and asthma research. Most fundamentally, exposure to common allergens, such as HDM, is nearly ubiquitous and T_H responses to these allergens are seen in both allergic and non-allergic subjects (33–35), yet why do only some people develop T_H2 responses to allergens? By comparing HDM-reactive T cells from asthmatics with and without HDM allergy (T_H2 responses versus no T_H2 responses), we found that in subjects without HDM allergy (but sensitized to other allergens, see table S1), a subset of T_H and T_{reg} cells expressing the interferon response signature was expanded. These cells expressed higher levels of TRAIL, a molecule that can inhibit TCR signaling, activation of T_H cells and inflammation in model systems (102). Therefore, we hypothesize that these TRAIL-expressing HDM-reactive T cells could play an important role in dampening T_H2 inflammation in allergy and asthma. A recent single-cell transcriptomic study identified T_H cells expressing the interferon response signature in the lung tissue of mice sensitized and challenged with HDM (20). This finding implies that T_HIFNR cells can be generated and sustained in vivo, and that HDM sensitization of mice may be an appropriate system to test the role of these cells in allergic inflammation. Future studies are also required to determine the molecular mechanisms and signals that drive the differentiation, maintenance, and persistence of T_HIFNR cells, ideally through the analysis of their molecular and chromatin landscape.

Another important question is why only some patients with allergy develop asthma? Do T_H cells from allergic patients with asthma display distinct molecular features from those of allergic patients without asthma? By comparing HDM-reactive T_H cells from allergic subjects with and without asthma, we defined a subset of *IL9*-expressing T_H2 cells that are

enriched in asthmatic subjects. We show that *IL9*-expressing HDM-reactive cells display several features likely to enhance their pathogenicity and persistence, which may contribute to asthma pathogenesis. Notably, in the context of peanut allergy, IL-9 was shown to best differentiate children with peanut allergy from children with peanut sensitization, who tolerate peanut, suggesting a potentially important role in food allergy (103). Studies blocking IL-9 activity in animal models of asthma have indicated that this may be a promising treatment approach (104, 105), but the relative importance of IL-9-producing T cells has not been fully explored. A recent report in cancer showed that IL-9-producing murine T_H cells are more cytolytic, hyperproliferative, and less exhausted (106, 107); these properties conferred potent antitumor activity for these cells when tested in adoptive transfer experiments. Studies in mouse models of allergic airway inflammation are required to demonstrate the relative pathogenicity and persistence of IL-9 producing T_H2 cells *in vivo*. Moreover, this cell population should also be characterized in human subjects with severe asthma, including those that reside in the airways. In summary, our single-cell transcriptomic study of HDM allergen-specific T cells has identified T_H subsets that may contribute to the pathogenesis of allergy and asthma.

Materials and Methods

Study design

The goal of this study was to use bulk and single-cell RNA-seq assay to capture the transcriptome of HDM allergen-reactive $CD4^+$ T cell memory subsets from peripheral blood mononuclear cells (PBMC) of 6 asthmatic subjects allergic to HDM, 6 asthmatic subjects non-allergic to HDM, 6 non-asthmatic subjects allergic to HDM, and 6 non-asthmatic non-allergic to HDM. To isolate HDM-reactive $CD4^+$ cells, PBMC were stimulated with HDM and $CD4^+$ memory cells were sorted based on CD154 and CD137 expression: $CD154^+$ (HDM-reactive T_H), $CD154^-$ $CD137^+$ (HDM-reactive T_{reg}), and $CD154^-$ $CD137^-$ (HDM-non-reactive T cells). For bulk RNA-seq, we collected 200 cells in triplicates, and for single-cell RNA-seq assay, we collected between 1,500 to 2,000 cells per cell type per patient (see table S1).

Subject recruitment, ethical approval and characteristics

Recruitment of subjects included in this study followed Institutional Review Board (La Jolla Institute for Immunology, La Jolla, CA) approval, and study participants gave written informed consent. Twelve non-smoking subjects with mild asthma treated only with inhaled bronchodilators (mild asthma), six subjects with allergic rhinitis but no asthma, meeting established diagnostic criteria, and 6 healthy nonatopic subjects were studied (Fig. 1A and table S1). Subjects with asthma underwent pulmonary function tests and/or methacholine challenge to establish diagnosis (bronchodilator response of ≥12 %, or ≥200 ml, and/or methacholine challenge with a provocative concentration causing a drop of the forced expiratory volume in 1 s [FEV1] of 20 %, 8 mg/ml). All subjects were classified as allergic to HDM based on skin test reactivity to HDM allergens (Der p and Der f, table S1).

Sample processing

We used peripheral blood mononuclear cells (PBMC) obtained from blood samples by density gradient centrifugation according to the manufacturer's instructions and cryopreserved in liquid nitrogen.

Antigen-reactive T cell enrichment (ARTE) assay

The HDM peptide pool was generated as described and contained 75 peptides at a total concentration of 20 mg/ml (188.7 ng/ml for each peptide) (108, 109). The assay to isolate HDM-reactive T cells based on HDM peptide pool stimulation, MACS-based enrichment and FACS sorting of $CD154^+$ memory $CD4^+$ T cells from PBMC was adapted from Bacher et al. 2016 (43), and is outlined in fig. S1. For each donor, PBMC cryovials were thawed, washed and, plated overnight in 6-well culture plates at a concentration of 10×10^6 cells/ml in 2 ml of serum-free TexMACS medium (Miltenyi Biotec) (5% CO_2, 37˚C). In presence of a blocking CD40 antibody (1 μg/ml; Miltenyi Biotec), cells were then stimulated by addition of HDM peptide pool (1 μg/ml) for 6 h. Subsequently, cells were stained with fluorescence-labeled antibodies and a biotinylated CD154 antibody (clone 5C8; Miltenyi Biotec). Anti-biotin microbeads (Miltenyi Biotec) were added to allow MACS-based enrichment of $CD154^+$ cells using MS columns (Miltenyi Biotec). 5% of cells were kept as control sample ('input') and used for FACS sorting of HDM^- T cells and analysis of cell frequencies before enrichment. Positively selected cells ($CD154^+$) were eluted from the column and used for FACS sorting of $CD154^+$ memory $CD4^+$ T cells. The flow-through from the MACS column was collected, stained with a biotinylated CD137 antibody (clone REA765; Miltenyi Biotec) and anti-biotin MicroBeads and applied to a second MS column. Positively selected cells ($CD137^+$) were used for FACS sorting of $CD137^+$ cells. All cell populations were FACS-sorted using a FACSAria II (Becton Dickinson); the gating strategy is shown in fig S1. All flow cytometry data were analyzed using FlowJo software (version 10).

Cell isolation for bulk and single-cell RNA-seq assay

For bulk assays, cells of interest were directly collected by sorting 200 cells into 0.2 ml PCR tubes (low-retention, Axygen) containing 8 μl of ice-cold lysis buffer (Triton X-100 [0.1 %, Sigma-Aldrich] containing RNase inhibitor (1:100, Takara). Once collected, tubes were vortexed for 10 seconds, spun for 1 minute at 3000 g and stored at −80 ˚C. For single cell RNA-seq assays (10x Genomics), 1000 to 2000 HDM-reactive T cells per subject were collected by sorting in low retention and sterile ice-cold 1.5 mL collection tubes containing 500 μL of PBS:FBS (1:1 vol:vol) with RNase inhibitor (1:100). HDM-reactive T cells from 6 subjects in each of the 4 groups (asthma with HDM-allergy, asthma without HDM allergy, HDM-allergy without asthma and healthy without HDM-allergy) were collected in the same tube. Collection tubes with ~9,000 to 12,000 sorted cells/study group were inverted a few times, ice-cold PBS was added to reach a volume of 1400 μl, and centrifugated for 5 minutes at a speed of 600 g at 4 ˚C. Supernatant was cautiously removed leaving 5 to 10 μl of volume. Pellets were then resuspended with 25 μl of 10x Genomics resuspension buffer (0.22 μm filtered ice-cold PBS supplemented with ultra-pure bovine serum albumin (0.04 %, Sigma-Aldrich). 33 μl of cell suspension were transferred to an 8 PCR-tube strip for downstream steps as per manufacturer's instructions (10x Genomics, San Francisco).

Bulk RNA library preparation for sequencing

For full-length bulk transcriptome analyses, we used the Smart-Seq2 protocol (110), adapted for samples with small cell numbers (111, 112). We followed the protocol as described previously (111, 112) with following modifications: (i) the pre-amplification PCR cycle for T cells was set at 22 cycles; (ii) to eliminate any traces of primer-dimers, the PCR pre-amplified cDNA product was purified using 0.8x Ampure-XP beads (Beckman Coulter) before using the DNA for sequencing library preparation. One ng of pre-amplified cDNA was used to generate barcoded Illumina sequencing libraries (Nextera XT library preparation kit, Illumina) in 8 μl reaction volume. Samples failing any quality control step (DNA quality assessed by capillary electrophoresis (Fragment analyzer, Advance analytical) and quantity (Picogreen quantification assay, Thermo Fisher) were eliminated from further downstream steps. Libraries were then pooled at equal molar concentration and sequenced using the HiSeq 2500 Illumina platform to obtain 50-bp single-end reads (HiSeq SBS Kit v4; Illumina). In total, 1.7 billion uniquely mapped reads we generated with a median ± standard deviation of 17.8 ± 3.8 million uniquely mapped reads per sample.

10x Genomics single-cell RNA library preparation for sequencing

Samples were processed using 10x Genomics 3'TAG v2 chemistry as per manufacturer's recommendations; 11 cycles were used for cDNA amplification and library preparation respectively (77). Barcoded RNA was collected and processed following manufacturer's recommendations. After quantification, equal molar concentration of each libraries was pooled and sequenced using the HiSeq2500 Illumina sequencing platform to obtain 26- and 100-bp paired-end reads using the following read length: read 1, 26 cycles; read 2, 100 cycles; and i7 index, 8 cycles.

Bulk RNA-seq analysis

Bulk RNA-seq data were mapped against the hg19 reference using TopHat (113) (v1.2.1 (--library-type fr-unstranded --no-coverage-search) with FastQC (v0.11.2), Bowtie (114) (v1.1.2), Samtools 0.1.18.0) (115) and we employed htseq-count -m union -s no -t exon -i gene_name (part of the HTSeq framework, version 0.7.1) (71, 116). Cutadapt (v1.3) was used to remove adapters (117). Values throughout are displayed as $\log_2$ TPM (transcripts per million) counts; a value of 1 was added prior to log transformation (pseudo-count). We performed principal component analysis and clustering analysis using t-distributed stochastic neighbor embedding dimensional reduction algorithm (tSNE) (118) (based on 3 PC using the top 200 most variable genes). To identify genes expressed differentially between groups, we performed negative binomial tests for paired comparisons by employing DESeq2 (119) (1.16.1) with default parameters. We considered genes to be expressed differentially by any comparison when the DESeq2 analysis resulted in a Benjamini-Hochberg–adjusted P-value of at most 0.01 and a $\log_2$ fold change of at least 2. Gene set enrichment analysis (GSEA) were performed as previously described (112, 120) using the Qlucore visualization software (version 3.5) (121). Gene lists used for GSEA analysis are shown in table S4.

Single-cell RNA-seq analysis

Analysis of 3' single-cell transcriptomes using the 10x Genomics platform: Raw data was processed as previously described (70, 77), merging multiple sequencing runs using count function from Cell Ranger (table S3), then aggregating multiple cell types with cell ranger aggr (v3.0.2). The merged data was transferred to the R statistical environment for analysis using the package Seurat (v3.0.2) (122).

Doublet cell filtering: Barcoded single-cell RNA-seq was demultiplexed patient-wise using Demuxlet (123) with the following parameters: alpha = 0, 0.5 and --geno-error = 0.05. Cells called as doublet by Demuxlet were removed from downstream analyses (fig. S3A and table S3). Identities were inferred by analyzing VCF files from the genotyping analysis containing the corresponding individual for each particular library. Each cell was assigned a donor ID or marked as a doublet, and then incorporated to the annotation table. We did not observe major changes in singlets/doublets proportion between the different 10x Genomics libraries (reflecting cell type and subject groups), suggesting optimal processing of cells during 10x (Gel Bead-In Emulsions) GEM generation and downstream steps (fig. S3A). All downstream analyses were performed using singlet cells.

Activation score and cell filtering: To filter out cells with low level of activation or no activation by the HDM-peptide pool i.e., HDM non-reactive cells, we performed pair-wise single-cell differential gene expression analysis using MAST algorithm (124) between HDM-reactive T_H cells ($CD154^+$ cells, N = 3075, random sampled) and HDM^- T cells ($CD154^{neg}$ cells, N = 3075). We defined a gene set (N = 110 genes, called HDM^+ T_H activation genes) that captured the transcripts upregulated in the $CD154^+$ versus $CD154^{neg}$ cells (table S3) using the following parameters (fig. S3B): Benjamini-Hochberg–adjusted P-value ≤ 0.05, $\log_2$ fold change ≥ 2, $\log_2$ mean of expression ≥ 0.75 CPM and, percentage of expressing cells (> 0 CPM) in HDM^+ T_H cells > 37.5 % (fig. S3B). We scored each cell using AddModuleScore from Seurat (122). Briefly, the module score is calculated by binning the genes by the average expression level, then the average expression of each gene is subtracted by the aggregated expression of the control gene sets (100) randomly selected per bin. Finally, based on the distribution of cells based on their activation score (Fig. 2A and fig. S3C), we applied a threshold for defining activated cells. The proportions of cells expressing important canonical genes such as *IL4*, *IL5*, *IFNG*, *IL17A* pre- and post-activation filtering indicated cell eliminated due to low-activation score did not upregulate transcripts for these genes (data not shown). Similarly, an independent HDM^+ T_{reg} activation score was also calculated using similar approach to analyze HDM^+ T_{reg} single-cell datasets (table S3 and fig. S3, right panels). In total, 3505 cells with low-activation score were eliminated from downstream analysis.

Transcriptome-based clustering analysis: The merged data was transferred to the R (v3.5) statistical environment for analysis using the package Seurat (v3.0.2) (122). Only cells expressing more than 200 genes and with a total mitochondrial gene expression less than 5 %, and genes expressed in at least 3 cells were included in the analysis. The data was then log-normalized per cell and a list of the most variable genes with a mean expression > 0.1 (UMI) and explaining 30 % of the cumulative standardized variance given by the

FindVariableFeatures function were used for clustering analysis (fig. S4). We performed clustering analysis using distinct lists of most variable genes for HDM$^+$ T_H, HDM$^+$ T_{REG} and HDM$^+$ T_H2 clusters (table S3). In regard to T_H2 sub-clustering, because of the limited number of cells, we considered most variable genes that were expressed by more than 10 % of the cells and with a standardized variance greater than 2. We also limited the selection of the most variable genes to 10 % of the cumulative standardized variance (fig. S4, right panels). Normalized single-cell transcriptomic data was then further scaled by the number of UMI-detected and percentage of mitochondrial reads. We then performed principal component (PC) analysis with RunPCA algorithm (122) using the determined most variable gene lists. We followed Seurat procedure to determine the number of PCs to select for downstream analyses, using the standard deviation of PCs. We applied FindNeighbors and FindClusters functions from Seurat with default settings (table S3 and fig. S4) to identify clusters. All clusters had more than 50 cells and none were excluded from the downstream analysis. Cluster specific markers were obtained by the FindAllMarkers function with default parameters, test.use = MAST (124). Further visualizations of exported normalized data such has “violin” plots were generated using the Seurat package and custom R scripts. Notably, our violin plots show Seurat normalized expression for a particular gene ($\log_2$ (CPM + 1 pseudo-count)) only for the cells expressing the gene of interest. Violin shape represents the distribution of cell expressing transcript of interest (based on a Gaussian Kernel density estimation model) and are colored according to the percentage of cell expressing the transcript of interest.

Single-cell differential gene expression analysis: Pairwise single-cell differential gene expression analysis was conducted after conversion of data to count per million base-pairs (CPM + 1) using MAST algorithm ($q < 0.05$, v1.2.1) (R package) (124). We used equal number of cells from each subject group, and random sampling performed when necessary. A gene was considered differentially expressed when Benjamini-Hochberg–adjusted P-value was < 0.05 and a $\log_2$ fold change was more than 0.25. For cluster-specific signatures, a gene was considered significantly different (unique to a group), only if the gene was enriched in every pair-wise comparison for a particular cluster with other clusters.

Single-cell co-expression analysis and weighted gene correlation analysis (WGCNA): In order to perform co-expression analysis, given the high levels of genes drop-out associated with single cell analysis, we performed a data imputation using SAVER imputation algorithm (125). Briefly, SAVER analysis was implemented on the Cell Ranger UMI matrix output for HDM$^+$ T_H using the function saver (v1.1.1) with pred.genes.only = TRUE. Then, we calculated Spearman correlations coefficients using the cor function and determined the cluster-modules through hclust on Euclidean distances and cutree functions k = 5 according to the within groups sums of squares elbow (similar to T_H single-cell clustering analysis, fig. S4). We also performed weighted correlation analysis using WGCNA algorithm (v1.66) (71) using the function TOMsimilarityfromExpr, power = 3, and exportNetworkToCytoscape, weighted = TRUE, threshold = 50th quantile of the topological overlap matrix. Network plots were generated by Gephi (0.9.2) using Fruchterman-Reingold and Noverlap layouts (126). The size and color of the nodes were defined according to the degree, while the edge width and color were scaled according to the weight value.

Genotyping

For each patient, genomic DNA was isolated from PBMC using the DNeasy Blood and Tissue Kit (Qiagen) and utilized for genotyping using the Infinium Multi-Ethnic Global-8 Kit (Illumina) following the manufacturer's instructions. Raw data from the genotyping analysis, data quality assessment and SNPs identification were performed as previously described (127).

Stimulation of memory CD4$^+$ T cells with human recombinant TRAIL

Memory CD4$^+$ T cells were isolated from PBMC using the Memory CD4$^+$ T Cell Isolation Kit (Miltenyi Biotec) and cultured in Iscove's Modified Dulbecco's Medium (IMDM; Invitrogen) supplemented with 5 % (vol/vol) heat-inactivated fetal bovine serum (FBS) and 2 % (vol/vol) human AB serum (CellGro). The memory CD4$^+$ T cells were stimulated with pre-coated human recombinant TRAIL (5 μg/ml), anti-CD3 antibodies (2.5 μg/ml) and soluble anti-CD28 antibodies (1 μg/ml) in presence of IL-7 (5 ng/ml; Miltenyi Biotec). The expression of surface markers (CD69, CD154, CD137) was analyzed by flow cytometry after 6 h.

Expression of TRAIL on memory CD4$^+$ T cells

Total PBMC were thawed, washed and plated overnight in serum-free TexMACS medium (Miltenyi Biotec) / complete IMDM (as described above). In presence of a blocking CD40 antibody (1 μg/ml in culture; clone HB14; Miltenyi Biotec), cells were then left untreated or stimulated by addition of the control reagent CytoStim (1:500 dilution of stock; Miltenyi Biotec). The expression of surface markers (CD69, CD154 and TRAIL) was analyzed by FACS after 6 h.

Statistical analysis

We used non-parametric Kruskal-Wallis one-way analysis of variance test (ANOVA) to compare unpaired data for more than 2 conditions and Kolmogoroz-Smirnov test when comparing 2 groups of data. We used paired Student's t-test for time-course flow cytometry analysis. We used GraphPad Prism 7.0. All source datasets and statistical used are detailed in table S5.

Supplementary Material

Refer to Web version on PubMed Central for supplementary material.

Acknowledgments

We thank Drs. C. Kim, D. Hinz and members of the flow cytometry core facility; Dr. J. Greenbaum and members of the Bioinformatics Core at La Jolla Institute for Immunology (LJI); Drs. A. Sette and B. Peters and their teams for graciously providing us with the pool of House Dust Mite peptides (108, 109); Mrs. J. Moore for assistance with manuscript and figure preparation; and the members of the Vijayanand, Sette and Peters labs for constructive intellectual and technical support. Finally, we thank all donors for their charitable contribution to academic research.

Funding: Supported by (i) NIH research grants: U19AI100275, U19AI135731, R01HL114093; (ii) NIH equipment grants: S10RR027366 (BD FACSAria II), S10 RR027366 (Illumina HiSeq 2500); (iii) the William K. Bowes Jr. Foundation (P.V.).

References and Notes

1. Caminati M, Pham DL, Bagnasco D, Canonica GW, Type 2 immunity in asthma. World Allergy Organ J 11, 13 (2018). [PubMed: 29988331]
2. Miller JD, The Role of Dust Mites in Allergy. Clin Rev Allergy Immunol 57, 312–329 (2019). [PubMed: 29936683]
3. Larche M, Akdis CA, Valenta R, Immunological mechanisms of allergen-specific immunotherapy. Nat Rev Immunol 6, 761–771 (2006). [PubMed: 16998509]
4. Kay AB, Allergy and allergic diseases. Second of two parts. N Engl J Med 344, 109–113 (2001). [PubMed: 11150362]
5. Kay AB, Allergy and allergic diseases. First of two parts. N Engl J Med 344, 30–37 (2001). [PubMed: 11136958]
6. Gregory LG, Lloyd CM, Orchestrating house dust mite-associated allergy in the lung. Trends Immunol 32, 402–411 (2011). [PubMed: 21783420]
7. Sykes A, Johnston SL, Etiology of asthma exacerbations. J Allergy Clin Immunol 122, 685–688 (2008). [PubMed: 19014758]
8. Oddera S, Silvestri M, Penna R, Galeazzi G, Crimi E, Rossi GA, Airway eosinophilic inflammation and bronchial hyperresponsiveness after allergen inhalation challenge in asthma. Lung 176, 237–247 (1998). [PubMed: 9617740]
9. Arshad SH, Hamilton RG, Adkinson NF Jr., Repeated aerosol exposure to small doses of allergen. A model for chronic allergic asthma. Am J Respir Crit Care Med 157, 1900–1906 (1998). [PubMed: 9620925]
10. Maestrelli P, Zanolla L, Puccinelli P, Pozzan M, Fabbri LM, Regione Veneto Study G, Low domestic exposure to house dust mite allergens (Der p 1) is associated with a reduced non-specific bronchial hyperresponsiveness in mite-sensitized asthmatic subjects under optimal drug treatment. Clin Exp Allergy 31, 715–721 (2001). [PubMed: 11422130]
11. Ali FR, Oldfield WL, Higashi N, Larche M, Kay AB, Late asthmatic reactions induced by inhalation of allergen-derived T cell peptides. Am J Respir Crit Care Med 169, 20–26 (2004). [PubMed: 14500264]
12. Muehling LM, Lawrence MG, Woodfolk JA, Pathogenic CD4(+) T cells in patients with asthma. J Allergy Clin Immunol 140, 1523–1540 (2017). [PubMed: 28442213]
13. Raemdonck K, Baker K, Dale N, Dubuis E, Shala F, Belvisi MG, Birrell MA, CD4(+) and CD8(+) T cells play a central role in a HDM driven model of allergic asthma. Respir Res 17, 45 (2016). [PubMed: 27112462]
14. Gibeon D, Menzies-Gow AN, Targeting interleukins to treat severe asthma. Expert Rev Respir Med 6, 423–439 (2012). [PubMed: 22971067]
15. Kim AS, Doherty TA, New and emerging therapies for asthma. Ann Allergy Asthma Immunol 116, 14–17 (2016). [PubMed: 26707770]
16. Maltby S, Gibson PG, Powell H, McDonald VM, Omalizumab Treatment Response in a Population With Severe Allergic Asthma and Overlapping COPD. Chest 151, 78–89 (2017). [PubMed: 27742181]
17. Drick N, Seeliger B, Welte T, Fuge J, Suhling H, Anti-IL-5 therapy in patients with severe eosinophilic asthma - clinical efficacy and possible criteria for treatment response. BMC Pulm Med 18, 119 (2018). [PubMed: 30021546]
18. Schulten V, Tripple V, Seumois G, Qian Y, Scheuermann RH, Fu Z, Locci M, Rosales S, Vijayanand P, Sette A, Alam R, Crotty S, Peters B, Allergen-specific immunotherapy modulates the balance of circulating Tfh and Tfr cells. J Allergy Clin Immunol 141, 775–777 e776 (2018). [PubMed: 28506846]
19. Noval Rivas M, Chatila TA, Regulatory T cells in allergic diseases. J Allergy Clin Immunol 138, 639–652 (2016). [PubMed: 27596705]
20. Tibbitt CA, Stark JM, Martens L, Ma J, Mold JE, Deswarte K, Oliynyk G, Feng X, Lambrecht BN, De Bleser P, Nylen S, Hammad H, Henriksson M. Arsenian, Saeys Y, Coquet JM, Single-Cell RNA Sequencing of the T Helper Cell Response to House Dust Mites Defines a Distinct Gene

Expression Signature in Airway Th2 Cells. Immunity 51, 169–184 e165 (2019). [PubMed: 31231035]

21. Lewkowich IP, Herman NS, Schleifer KW, Dance MP, Chen BL, Dienger KM, Sproles AA, Shah JS, Kohl J, Belkaid Y, Wills-Karp M, CD4+CD25+ T cells protect against experimentally induced asthma and alter pulmonary dendritic cell phenotype and function. J Exp Med 202, 1549–1561 (2005). [PubMed: 16314437]
22. Leech MD, Benson RA, De Vries A, Fitch PM, Howie SE, Resolution of Der p1-induced allergic airway inflammation is dependent on CD4+CD25+Foxp3+ regulatory cells. J Immunol 179, 7050–7058 (2007). [PubMed: 17982096]
23. Strickland DH, Stumbles PA, Zosky GR, Subrata LS, Thomas JA, Turner DJ, Sly PD, Holt PG, Reversal of airway hyperresponsiveness by induction of airway mucosal CD4+CD25+ regulatory T cells. J Exp Med 203, 2649–2660 (2006). [PubMed: 17088431]
24. Wambre E, Bajzik V, DeLong JH, O'Brien K, Nguyen QA, Speake C, Gersuk VH, DeBerg HA, Whalen E, Ni C, Farrington M, Jeong D, Robinson D, Linsley PS, Vickery BP, Kwok WW, A phenotypically and functionally distinct human TH2 cell subpopulation is associated with allergic disorders. Sci Transl Med 9, (2017).
25. Smith KA, Gray NJ, Saleh F, Cheek E, Frew AJ, Kern F, Tarzi MD, Characterisation of CD154+ T cells following ex vivo allergen stimulation illustrates distinct T cell responses to seasonal and perennial allergens in allergic and non-allergic individuals. BMC Immunol 14, 49 (2013). [PubMed: 24188324]
26. Upadhyaya B, Yin Y, Hill BJ, Douek DC, Prussin C, Hierarchical IL-5 expression defines a subpopulation of highly differentiated human Th2 cells. J Immunol 187, 3111–3120 (2011). [PubMed: 21849680]
27. Januszyk M, Rennert RC, Sorkin M, Maan ZN, Wong LK, Whittam AJ, Whitmore A, Duscher D, Gurtner GC, Evaluating the Effect of Cell Culture on Gene Expression in Primary Tissue Samples Using Microfluidic-Based Single Cell Transcriptional Analysis. Microarrays (Basel) 4, 540–550 (2015). [PubMed: 27600239]
28. Nestor CE, Ottaviano R, Reinhardt D, Cruickshanks HA, Mjoseng HK, McPherson RC, Lentini A, Thomson JP, Dunican DS, Pennings S, Anderton SM, Benson M, Meehan RR, Rapid reprogramming of epigenetic and transcriptional profiles in mammalian culture systems. Genome Biol 16, 11 (2015). [PubMed: 25648825]
29. Mazzatti DJ, White A, Forsey RJ, Powell JR, Pawelec G, Gene expression changes in long-term culture of T-cell clones: genomic effects of chronic antigenic stress in aging and immunosenescence. Aging Cell 6, 155–163 (2007). [PubMed: 17286612]
30. Seumois G, Zapardiel-Gonzalo J, White B, Singh D, Schulten V, Dillon M, Hinz D, Broide DH, Sette A, Peters B, Vijayanand P, Transcriptional Profiling of Th2 Cells Identifies Pathogenic Features Associated with Asthma. J Immunol 197, 655–664 (2016). [PubMed: 27271570]
31. Geginat J, Paroni M, Maglie S, Alfen JS, Kastirr I, Gruarin P, De Simone M, Pagani M, Abrignani S, Plasticity of human CD4 T cell subsets. Front Immunol 5, 630 (2014). [PubMed: 25566245]
32. DuPage M, Bluestone JA, Harnessing the plasticity of CD4(+) T cells to treat immune-mediated disease. Nat Rev Immunol 16, 149–163 (2016). [PubMed: 26875830]
33. Hinz D, Seumois G, Gholami AM, Greenbaum JA, Lane J, White B, Broide DH, Schulten V, Sidney J, Bakhru P, Oseroff C, Wambre E, James EA, Kwok WW, Peters B, Vijayanand P, Sette A, Lack of allergy to timothy grass pollen is not a passive phenomenon but associated with the allergen-specific modulation of immune reactivity. Clin Exp Allergy 46, 705–719 (2016). [PubMed: 26662458]
34. Birrueta G, Tripple V, Pham J, Manohar M, James EA, Kwok WW, Nadeau KC, Sette A, Peters B, Schulten V, Peanut-specific T cell responses in patients with different clinical reactivity. PLoS One 13, e0204620 (2018). [PubMed: 30304054]
35. Schulten V, Westernberg L, Birrueta G, Sidney J, Paul S, Busse P, Peters B, Sette A, Allergen and Epitope Targets of Mouse-Specific T Cell Responses in Allergy and Asthma. Front Immunol 9, 235 (2018). [PubMed: 29487600]
36. Akdis M, Verhagen J, Taylor A, Karamloo F, Karagiannidis C, Crameri R, Thunberg S, Deniz G, Valenta R, Fiebig H, Kegel C, Disch R, Schmidt-Weber CB, Blaser K, Akdis CA, Immune

responses in healthy and allergic individuals are characterized by a fine balance between allergen-specific T regulatory 1 and T helper 2 cells. J Exp Med 199, 1567–1575 (2004). [PubMed: 15173208]

37. Gandhi VD, Davidson C, Asaduzzaman M, Nahirney D, Vliagoftis H, House dust mite interactions with airway epithelium: role in allergic airway inflammation. Curr Allergy Asthma Rep 13, 262–270 (2013). [PubMed: 23585216]
38. Calderon MA, Kleine-Tebbe J, Linneberg A, De Blay F, Hernandez D Fernandez de Rojas, J. C. Virchow, P. Demoly, House Dust Mite Respiratory Allergy: An Overview of Current Therapeutic Strategies. J Allergy Clin Immunol Pract 3, 843–855 (2015). [PubMed: 26342746]
39. Dullaers M, Schuijs MJ, Willart M, Fierens K, Van Moorleghem J, Hammad H, Lambrecht BN, House dust mite-driven asthma and allergen-specific T cells depend on B cells when the amount of inhaled allergen is limiting. J Allergy Clin Immunol 140, 76–88 e77 (2017). [PubMed: 27746238]
40. Salo PM, Arbes SJ Jr., Crockett PW, Thorne PS, Cohn RD, Zeldin DC, Exposure to multiple indoor allergens in US homes and its relationship to asthma. J Allergy Clin Immunol 121, 678–684 e672 (2008). [PubMed: 18255132]
41. Frentsch M, Arbach O, Kirchhoff D, Moewes B, Worm M, Rothe M, Scheffold A, Thiel A, Direct access to CD4+ T cells specific for defined antigens according to CD154 expression. Nat Med 11, 1118–1124 (2005). [PubMed: 16186818]
42. Chattopadhyay PK, Yu J, Roederer M, A live-cell assay to detect antigen-specific CD4+ T cells with diverse cytokine profiles. Nat Med 11, 1113–1117 (2005). [PubMed: 16186817]
43. Bacher P, Heinrich F, Stervbo U, Nienen M, Vahldieck M, Iwert C, Vogt K, Kollet J, Babel N, Sawitzki B, Schwarz C, Bereswill S, Heimesaat MM, Heine G, Gadermaier G, Asam C, Assenmacher M, Kniemeyer O, Brakhage AA, Ferreira F, Wallner M, Worm M, Scheffold A, Regulatory T Cell Specificity Directs Tolerance versus Allergy against Aeroantigens in Humans. Cell 167, 1067–1078 e1016 (2016). [PubMed: 27773482]
44. Arlehamn CL, Seumois G, Gerasimova A, Huang C, Fu Z, Yue X, Sette A, Vijayanand P, Peters B, Transcriptional profile of tuberculosis antigen-specific T cells reveals novel multifunctional features. J Immunol 193, 2931–2940 (2014). [PubMed: 25092889]
45. Serroukh Y, Gu-Trantien C, Hooshiar Kashani B, Defrance M, Vu Manh TP, Azouz A, Detavernier A, Hoyois A, Das J, Bizet M, Pollet E, Tabbuso T, Calonne E, van Gisbergen K, Dalod M, Fuks F, Goriely S, Marchant A, The transcription factors Runx3 and ThPOK cross-regulate acquisition of cytotoxic function by human Th1 lymphocytes. Elife 7, (2018).
46. Kroczek AL, Hartung E, Gurka S, Becker M, Reeg N, Mages HW, Voigt S, Freund C, Kroczek RA, Structure-Function Relationship of XCL1 Used for in vivo Targeting of Antigen Into XCR1(+) Dendritic Cells. Front Immunol 9, 2806 (2018). [PubMed: 30619244]
47. Dorner BG, Scheffold A, Rolph MS, Huser MB, Kaufmann SH, Radbruch A, Flesch IE, Kroczek RA, MIP-1alpha, MIP-1beta, RANTES, and ATAC/lymphotactin function together with IFN-gamma as type 1 cytokines. Proc Natl Acad Sci U S A 99, 6181–6186 (2002). [PubMed: 11972057]
48. Yoshida T, Imai T, Kakizaki M, Nishimura M, Takagi S, Yoshie O, Identification of single C motif-1/lymphotactin receptor XCR1. J Biol Chem 273, 16551–16554 (1998). [PubMed: 9632725]
49. Haider AS, Cardinale IR, Whynot JA, Krueger JG, Effects of etanercept are distinct from infliximab in modulating proinflammatory genes in activated human leukocytes. J Investig Dermatol Symp Proc 12, 9–15 (2007).
50. Liang SC, Tan XY, Luxenberg DP, Karim R, Dunussi-Joannopoulos K, Collins M, Fouser LA, Interleukin (IL)-22 and IL-17 are coexpressed by Th17 cells and cooperatively enhance expression of antimicrobial peptides. J Exp Med 203, 2271–2279 (2006). [PubMed: 16982811]
51. Lee Y, Awasthi A, Yosef N, Quintana FJ, Xiao S, Peters A, Wu C, Kleinewietfeld M, Kunder S, Hafler DA, Sobel RA, Regev A, Kuchroo VK, Induction and molecular signature of pathogenic TH17 cells. Nat Immunol 13, 991–999 (2012). [PubMed: 22961052]
52. Ramesh R, Kozhaya L, McKevitt K, Djuretic IM, Carlson TJ, Quintero MA, McCauley JL, Abreu MT, Unutmaz D, Sundrud MS, Pro-inflammatory human Th17 cells selectively express P-glycoprotein and are refractory to glucocorticoids. J Exp Med 211, 89–104 (2014). [PubMed: 24395888]

53. Liu SY, Sanchez DJ, Aliyari R, Lu S, Cheng G, Systematic identification of type I and type II interferon-induced antiviral factors. Proc Natl Acad Sci U S A 109, 4239–4244 (2012). [PubMed: 22371602]
54. Lee AJ, Ashkar AA, The Dual Nature of Type I and Type II Interferons. Front Immunol 9, 2061 (2018). [PubMed: 30254639]
55. Georas SN, Guo J, De Fanis U, Casolaro V, T-helper cell type-2 regulation in allergic disease. Eur Respir J 26, 1119–1137 (2005). [PubMed: 16319345]
56. Corry DB, Kheradmand F, Induction and regulation of the IgE response. Nature 402, B18–23 (1999). [PubMed: 10586891]
57. Oettgen HC, Geha RS, IgE in asthma and atopy: cellular and molecular connections. J Clin Invest 104, 829–835 (1999). [PubMed: 10510320]
58. Li J, Ge M, Lu S, Shi J, Li X, Wang M, Huang J, Shao Y, Huang Z, Zhang J, Nie N, Zheng Y, Pro-inflammatory effects of the Th1 chemokine CXCL10 in acquired aplastic anaemia. Cytokine 94, 45–51 (2017). [PubMed: 28411045]
59. Gauthier M, Chakraborty K, Oriss TB, Raundhal M, Das S, Chen J, Huff R, Sinha A, Fajt M, Ray P, Wenzel SE, Ray A, Severe asthma in humans and mouse model suggests a CXCL10 signature underlies corticosteroid-resistant Th1 bias. JCI Insight 2, (2017).
60. Groom JR, Richmond J, Murooka TT, Sorensen EW, Sung JH, Bankert K, von Andrian UH, Moon JJ, Mempel TR, Luster AD, CXCR3 chemokine receptor-ligand interactions in the lymph node optimize CD4+ T helper 1 cell differentiation. Immunity 37, 1091–1103 (2012). [PubMed: 23123063]
61. Beyer K, Baukloh AK, Stoyanova A, Kamphues C, Sattler A, Kotsch K, Interactions of Tumor Necrosis Factor-Related Apoptosis-Inducing Ligand (TRAIL) with the Immune System: Implications for Inflammation and Cancer. Cancers (Basel) 11, (2019).
62. Peteranderl C, Herold S, The Impact of the Interferon/TNF-Related Apoptosis-Inducing Ligand Signaling Axis on Disease Progression in Respiratory Viral Infection and Beyond. Front Immunol 8, 313 (2017). [PubMed: 28382038]
63. Lehnert C, Weiswange M, Jeremias I, Bayer C, Grunert M, Debatin KM, Strauss G, TRAIL-receptor costimulation inhibits proximal TCR signaling and suppresses human T cell activation and proliferation. J Immunol 193, 4021–4031 (2014). [PubMed: 25217163]
64. Chyuan IT, Tsai HF, Wu CS, Sung CC, Hsu PN, TRAIL-Mediated Suppression of T Cell Receptor Signaling Inhibits T Cell Activation and Inflammation in Experimental Autoimmune Encephalomyelitis. Front Immunol 9, 15 (2018). [PubMed: 29403497]
65. Roberts AI, Devadas S, Zhang X, Zhang L, Keegan A, Greeneltch K, Solomon J, Wei L, Das J, Sun E, Liu C, Yuan Z, Zhou JN, Shi Y, The role of activation-induced cell death in the differentiation of T-helper-cell subsets. Immunol Res 28, 285–293 (2003). [PubMed: 14713720]
66. Zhang XR, Zhang LY, Devadas S, Li L, Keegan AD, Shi YF, Reciprocal expression of TRAIL and CD95L in Th1 and Th2 cells: role of apoptosis in T helper subset differentiation. Cell Death Differ 10, 203–210 (2003). [PubMed: 12700648]
67. Guo X, Zhang Y, Zheng L, Zheng C, Song J, Zhang Q, Kang B, Liu Z, Jin L, Xing R, Gao R, Zhang L, Dong M, Hu X, Ren X, Kirchhoff D, Roider HG, Yan T, Zhang Z, Global characterization of T cells in non-small-cell lung cancer by single-cell sequencing. Nat Med 24, 978–985 (2018). [PubMed: 29942094]
68. Bacher P, Schink C, Teutschbein J, Kniemeyer O, Assenmacher M, Brakhage AA, Scheffold A, Antigen-reactive T cell enrichment for direct, high-resolution analysis of the human naive and memory Th cell repertoire. J Immunol 190, 3967–3976 (2013). [PubMed: 23479226]
69. van Dam S, Vosa U, van der Graaf A, Franke L, de Magalhaes JP, Gene co-expression analysis for functional classification and gene-disease predictions. Brief Bioinform 19, 575–592 (2018). [PubMed: 28077403]
70. Clarke J, Panwar B, Madrigal A, Singh D, Gujar R, Wood O, Chee SJ, Eschweiler S, King EV, Awad AS, Hanley CJ, McCann KJ, Bhattacharyya S, Woo E, Alzetani A, Seumois G, Thomas GJ, Ganesan AP, Friedmann PS, Sanchez-Elsner T, Ay F, Ottensmeier CH, Vijayanand P, Single-cell transcriptomic analysis of tissue-resident memory T cells in human lung cancer. J Exp Med 216, 2128–2149 (2019). [PubMed: 31227543]

71. Langfelder P, Horvath S, WGCNA: an R package for weighted correlation network analysis. BMC Bioinformatics 9, 559 (2008). [PubMed: 19114008]
72. Huber M, Lohoff M, IRF4 at the crossroads of effector T-cell fate decision. Eur J Immunol 44, 1886–1895 (2014). [PubMed: 24782159]
73. Ahlfors H, Limaye A, Elo LL, Tuomela S, Burute M, Gottimukkala KV, Notani D, Rasool O, Galande S, Lahesmaa R, SATB1 dictates expression of multiple genes including IL-5 involved in human T helper cell differentiation. Blood 116, 1443–1453 (2010). [PubMed: 20522714]
74. O'Garra A, Gabrysova L, Transcription Factors Directing Th2 Differentiation: Gata-3 Plays a Dominant Role. J Immunol 196, 4423–4425 (2016). [PubMed: 27207804]
75. Micosse C, von Meyenn L, Steck O, Kipfer E, Adam C, Simillion C, Seyed Jafari SM, Olah P, Yawlkar N, Simon D, Borradori L, Kuchen S, Yerly D, Homey B, Conrad C, Snijder B, Schmidt M, Schlapbach C, Human "TH9" cells are a subpopulation of PPAR-gamma(+) TH2 cells. Sci Immunol 4, (2019).
76. Prakash MD, Munoz MA, Jain R, Tong PL, Koskinen A, Regner M, Kleifeld O, Ho B, Olson M, Turner SJ, Mrass P, Weninger W, Bird PI, Granzyme B promotes cytotoxic lymphocyte transmigration via basement membrane remodeling. Immunity 41, 960–972 (2014). [PubMed: 25526309]
77. Patil VS, Madrigal A, Schmiedel BJ, Clarke J, O'Rourke P, de Silva AD, Harris E, Peters B, Seumois G, Weiskopf D, Sette A, Vijayanand P, Precursors of human CD4(+) cytotoxic T lymphocytes identified by single-cell transcriptome analysis. Sci Immunol 3, (2018).
78. Stinchcombe JC, Barral DC, Mules EH, Booth S, Hume AN, Machesky LM, Seabra MC, Griffiths GM, Rab27a is required for regulated secretion in cytotoxic T lymphocytes. J Cell Biol 152, 825–834 (2001). [PubMed: 11266472]
79. Omilusik KD, Best JA, Yu B, Goossens S, Weidemann A, Nguyen JV, Seuntjens E, Stryjewska A, Zweier C, Roychoudhuri R, Gattinoni L, Bird LM, Higashi Y, Kondoh H, Huylebroeck D, Haigh J, Goldrath AW, Transcriptional repressor ZEB2 promotes terminal differentiation of CD8+ effector and memory T cell populations during infection. J Exp Med 212, 2027–2039 (2015). [PubMed: 26503445]
80. Marshall NB, Swain SL, Cytotoxic CD4 T cells in antiviral immunity. J Biomed Biotechnol 2011, 954602 (2011). [PubMed: 22174559]
81. Thewissen M, Somers V, Hellings N, Fraussen J, Damoiseaux J, Stinissen P, CD4+CD28null T cells in autoimmune disease: pathogenic features and decreased susceptibility to immunoregulation. J Immunol 179, 6514–6523 (2007). [PubMed: 17982040]
82. Takamori A, Nambu A, Sato K, Yamaguchi S, Matsuda K, Numata T, Sugawara T, Yoshizaki T, Arae K, Morita H, Matsumoto K, Sudo K, Okumura K, Kitaura J, Matsuda H, Nakae S, IL-31 is crucial for induction of pruritus, but not inflammation, in contact hypersensitivity. Sci Rep 8, 6639 (2018). [PubMed: 29703903]
83. Gibbs BF, Patsinakidis N, Raap U, Role of the Pruritic Cytokine IL-31 in Autoimmune Skin Diseases. Front Immunol 10, 1383 (2019). [PubMed: 31281316]
84. Schroeder JT, Chichester KL, Bieneman AP, Human basophils secrete IL-3: evidence of autocrine priming for phenotypic and functional responses in allergic disease. J Immunol 182, 2432–2438 (2009). [PubMed: 19201898]
85. Williams GT, Smith CA, Spooncer E, Dexter TM, Taylor DR, Haemopoietic colony stimulating factors promote cell survival by suppressing apoptosis. Nature 343, 76–79 (1990). [PubMed: 1688645]
86. Weber GF, Chousterman BG, He S, Fenn AM, Nairz M, Anzai A, Brenner T, Uhle F, Iwamoto Y, Robbins CS, Noiret L, Maier SL, Zonnchen T, Rahbari NN, Scholch S, Klotzsche-von Ameln A, Chavakis T, Weitz J, Hofer S, Weigand MA, Nahrendorf M, Weissleder R, Swirski FK, Interleukin-3 amplifies acute inflammation and is a potential therapeutic target in sepsis. Science 347, 1260–1265 (2015). [PubMed: 25766237]
87. Nelson RK, Brickner H, Panwar B, Ramirez-Suastegui C, Herrera-de la Mata S, Liu N, Diaz D, Alexander LEC, Ay F, Vijayanand P, Seumois G, Akuthota P, Human Eosinophils Express a Distinct Gene Expression Program in Response to IL-3 Compared with Common beta-Chain Cytokines IL-5 and GM-CSF. J Immunol 203, 329–337 (2019). [PubMed: 31175163]

88. Chen L, Flies DB, Molecular mechanisms of T cell co-stimulation and co-inhibition. Nat Rev Immunol 13, 227–242 (2013). [PubMed: 23470321]

89. Oh H, Ghosh S, NF-kappaB: roles and regulation in different CD4(+) T-cell subsets. Immunol Rev 252, 41–51 (2013). [PubMed: 23405894]

90. Mandal M, Borowski C, Palomero T, Ferrando AA, Oberdoerffer P, Meng F, Ruiz-Vela A, Ciofani M, Zuniga-Pflucker JC, Screpanti I, Look AT, Korsmeyer SJ, Rajewsky K, von Boehmer H, Aifantis I, The BCL2A1 gene as a pre-T cell receptor-induced regulator of thymocyte survival. J Exp Med 201, 603–614 (2005). [PubMed: 15728238]

91. Sarkar SA, Kutlu B, Velmurugan K, Kizaka-Kondoh S, Lee CE, Wong R, Valentine A, Davidson HW, Hutton JC, Pugazhenthi S, Cytokine-mediated induction of anti-apoptotic genes that are linked to nuclear factor kappa-B (NF-kappaB) signalling in human islets and in a mouse beta cell line. Diabetologia 52, 1092–1101 (2009). [PubMed: 19343319]

92. Lawan A, Al-Harthi S, Cadalbert L, McCluskey AG, Shweash M, Grassia G, Grant A, Boyd M, Currie S, Plevin R, Deletion of the dual specific phosphatase-4 (DUSP-4) gene reveals an essential non-redundant role for MAP kinase phosphatase-2 (MKP-2) in proliferation and cell survival. J Biol Chem 286, 12933–12943 (2011). [PubMed: 21317287]

93. Al-Mutairi MS, Cadalbert LC, McGachy HA, Shweash M, Schroeder J, Kurnik M, Sloss CM, Bryant CE, Alexander J, Plevin R, MAP kinase phosphatase-2 plays a critical role in response to infection by Leishmania mexicana. PLoS Pathog 6, e1001192 (2010). [PubMed: 21085614]

94. Tseveleki V, Bauer J, Taoufik E, Ruan C, Leondiadis L, Haralambous S, Lassmann H, Probert L, Cellular FLIP (long isoform) overexpression in T cells drives Th2 effector responses and promotes immunoregulation in experimental autoimmune encephalomyelitis. J Immunol 173, 6619–6626 (2004). [PubMed: 15557152]

95. Lohning M, Stroehmann A, Coyle AJ, Grogan JL, Lin S, Gutierrez-Ramos JC, Levinson D, Radbruch A, Kamradt T, T1/ST2 is preferentially expressed on murine Th2 cells, independent of interleukin 4, interleukin 5, and interleukin 10, and important for Th2 effector function. Proc Natl Acad Sci U S A 95, 6930–6935 (1998). [PubMed: 9618516]

96. Alvarez F, Fritz JH, Piccirillo CA, Pleiotropic Effects of IL-33 on CD4(+) T Cell Differentiation and Effector Functions. Front Immunol 10, 522 (2019). [PubMed: 30949175]

97. Finnson KW, Tam BY, Liu K, Marcoux A, Lepage P, Roy S, Bizet AA, Philip A, Identification of CD109 as part of the TGF-beta receptor system in human keratinocytes. FASEB J 20, 1525–1527 (2006). [PubMed: 16754747]

98. Stritesky GL, Muthukrishnan R, Sehra S, Goswami R, Pham D, Travers J, Nguyen ET, Levy DE, Kaplan MH, The transcription factor STAT3 is required for T helper 2 cell development. Immunity 34, 39–49 (2011). [PubMed: 21215659]

99. Chuang CH, Greenside PG, Rogers ZN, Brady JJ, Yang D, Ma RK, Caswell DR, Chiou SH, Winters AF, Gruner BM, Ramaswami G, Spencley AL, Kopecky KE, Sayles LC, Sweet-Cordero EA, Li JB, Kundaje A, Winslow MM, Molecular definition of a metastatic lung cancer state reveals a targetable CD109-Janus kinase-Stat axis. Nat Med 23, 291–300 (2017). [PubMed: 28191885]

100. Litvinov IV, Bizet AA, Binamer Y, Jones DA, Sasseville D, Philip A, CD109 release from the cell surface in human keratinocytes regulates TGF-beta receptor expression, TGF-beta signalling and STAT3 activation: relevance to psoriasis. Exp Dermatol 20, 627–632 (2011). [PubMed: 21539622]

101. Gavino AC, Nahmod K, Bharadwaj U, Makedonas G, Tweardy DJ, STAT3 inhibition prevents lung inflammation, remodeling, and accumulation of Th2 and Th17 cells in a murine asthma model. Allergy 71, 1684–1692 (2016). [PubMed: 27225906]

102. Chyuan IT, Tsai HF, Wu CS, Hsu PN, TRAIL suppresses gut inflammation and inhibits colitogeic T-cell activation in experimental colitis via an apoptosis-independent pathway. Mucosal Immunol 12, 980–989 (2019). [PubMed: 31076664]

103. Brough HA, Cousins DJ, Munteanu A, Wong YF, Sudra A, Makinson K, Stephens AC, Arno M, Ciortuz L, Lack G, Turcanu V, IL-9 is a key component of memory TH cell peanut-specific responses from children with peanut allergy. J Allergy Clin Immunol 134, 1329–1338 e1310 (2014). [PubMed: 25112699]

104. Gong F, Pan YH, Huang X, Zhu HY, Jiang DL, From bench to bedside: Therapeutic potential of interleukin-9 in the treatment of asthma. Exp Ther Med 13, 389–394 (2017). [PubMed: 28352305]
105. Oh CK, Leigh R, McLaurin KK, Kim K, Hultquist M, Molfino NA, A randomized, controlled trial to evaluate the effect of an anti-interleukin-9 monoclonal antibody in adults with uncontrolled asthma. Respir Res 14, 93 (2013). [PubMed: 24050312]
106. Lu Y, Hong B, Li H, Zheng Y, Zhang M, Wang S, Qian J, Yi Q, Tumor-specific IL-9-producing CD8+ Tc9 cells are superior effector than type-I cytotoxic Tc1 cells for adoptive immunotherapy of cancers. Proc Natl Acad Sci U S A 111, 2265–2270 (2014). [PubMed: 24469818]
107. Xue G, Jin G, Fang J, Lu Y, IL-4 together with IL-1beta induces antitumor Th9 cell differentiation in the absence of TGF-beta signaling. Nat Commun 10, 1376 (2019). [PubMed: 30914642]
108. Hinz D, Oseroff C, Pham J, Sidney J, Peters B, Sette A, Definition of a pool of epitopes that recapitulates the T cell reactivity against major house dust mite allergens. Clin Exp Allergy 45, 1601–1612 (2015). [PubMed: 25652035]
109. Oseroff C, Christensen LH, Westernberg L, Pham J, Lane J, Paul S, Greenbaum J, Stranzl T, Lund G, Hoof I, Holm J, Wurtzen PA, Meno KH, Frazier A, Schulten V, Andersen PS, Peters B, Sette A, Immunoproteomic analysis of house dust mite antigens reveals distinct classes of dominant T cell antigens according to function and serological reactivity. Clin Exp Allergy 47, 577–592 (2017). [PubMed: 27684489]
110. Picelli S, Bjorklund AK, Faridani OR, Sagasser S, Winberg G, Sandberg R, Smart-seq2 for sensitive full-length transcriptome profiling in single cells. Nat Methods 10, 1096–1098 (2013). [PubMed: 24056875]
111. Rosales SL, Liang S, Engel I, Schmiedel BJ, Kronenberg M, Vijayanand P, Seumois G, A Sensitive and Integrated Approach to Profile Messenger RNA from Samples with Low Cell Numbers. Methods Mol Biol 1799, 275–301 (2018). [PubMed: 29956159]
112. Engel I, Seumois G, Chavez L, Samaniego-Castruita D, White B, Chawla A, Mock D, Vijayanand P, Kronenberg M, Innate-like functions of natural killer T cell subsets result from highly divergent gene programs. Nat Immunol 17, 728–739 (2016). [PubMed: 27089380]
113. Trapnell C, Pachter L, Salzberg SL, TopHat: discovering splice junctions with RNA-Seq. Bioinformatics 25, 1105–1111 (2009). [PubMed: 19289445]
114. Langmead B, Trapnell C, Pop M, Salzberg SL, Ultrafast and memory-efficient alignment of short DNA sequences to the human genome. Genome Biol 10, R25 (2009). [PubMed: 19261174]
115. Li H, Durbin R, Fast and accurate short read alignment with Burrows-Wheeler transform. Bioinformatics 25, 1754–1760 (2009). [PubMed: 19451168]
116. Anders S, Pyl PT, Huber W, HTSeq--a Python framework to work with high-throughput sequencing data. Bioinformatics 31, 166–169 (2015). [PubMed: 25260700]
117. Martin M, Cutadapt Removes Adapter Sequences From High-Throughput Sequencing Reads. EMBnet.Journal 17, 10–12 (2011).
118. van der Maaten L, Accelerating t-SNE using Tree-Based Algorithms. Journal of Machine Learning Research 15, 3221–3245 (2014).
119. Love MI, Huber W, Anders S, Moderated estimation of fold change and dispersion for RNA-seq data with DESeq2. Genome Biol 15, 550 (2014). [PubMed: 25516281]
120. Ganesan AP, Clarke J, Wood O, Garrido-Martin EM, Chee SJ, Mellows T, Samaniego-Castruita D, Singh D, Seumois G, Alzetani A, Woo E, Friedmann PS, King EV, Thomas GJ, Sanchez-Elsner T, Vijayanand P, Ottensmeier CH, Tissue-resident memory features are linked to the magnitude of cytotoxic T cell responses in human lung cancer. Nat Immunol 18, 940–950 (2017). [PubMed: 28628092]
121. Subramanian A, Tamayo P, Mootha VK, Mukherjee S, Ebert BL, Gillette MA, Paulovich A, Pomeroy SL, Golub TR, Lander ES, Mesirov JP, Gene set enrichment analysis: a knowledge-based approach for interpreting genome-wide expression profiles. Proc Natl Acad Sci U S A 102, 15545–15550 (2005). [PubMed: 16199517]
122. Stuart T, Butler A, Hoffman P, Hafemeister C, Papalexi E, Mauck WM 3rd, Hao Y, Stoeckius M, Smibert P, Satija R, Comprehensive Integration of Single-Cell Data. Cell 177, 1888–1902 e1821 (2019). [PubMed: 31178118]

123. Kang HM, Subramaniam M, Targ S, Nguyen M, Maliskova L, McCarthy E, Wan E, Wong S, Byrnes L, Lanata CM, Gate RE, Mostafavi S, Marson A, Zaitlen N, Criswell LA, Ye CJ, Multiplexed droplet single-cell RNA-sequencing using natural genetic variation. Nat Biotechnol 36, 89–94 (2018). [PubMed: 29227470]

124. Finak G, McDavid A, Yajima M, Deng J, Gersuk V, Shalek AK, Slichter CK, Miller HW, McElrath MJ, Prlic M, Linsley PS, Gottardo R, MAST: a flexible statistical framework for assessing transcriptional changes and characterizing heterogeneity in single-cell RNA sequencing data. Genome Biol 16, 278 (2015). [PubMed: 26653891]

125. Huang M, Wang J, Torre E, Dueck H, Shaffer S, Bonasio R, Murray JI, Raj A, Li M, Zhang NR, SAVER: gene expression recovery for single-cell RNA sequencing. Nat Methods 15, 539–542 (2018). [PubMed: 29941873]

126. Bastian M, Heymann S, Jacomy M, Gephi: An Open Source Software for Exploring and Manipulating Networks. 2009 (2009).

127. Schmiedel BJ, Singh D, Madrigal A, Valdovino-Gonzalez AG, White BM, Zapardiel-Gonzalo J, Ha B, Altay G, Greenbaum JA, McVicker G, Seumois G, Rao A, Kronenberg M, Peters B, Vijayanand P, Impact of Genetic Polymorphisms on Human Immune Cell Gene Expression. Cell 175, 1701–1715 e1716 (2018). [PubMed: 30449622]

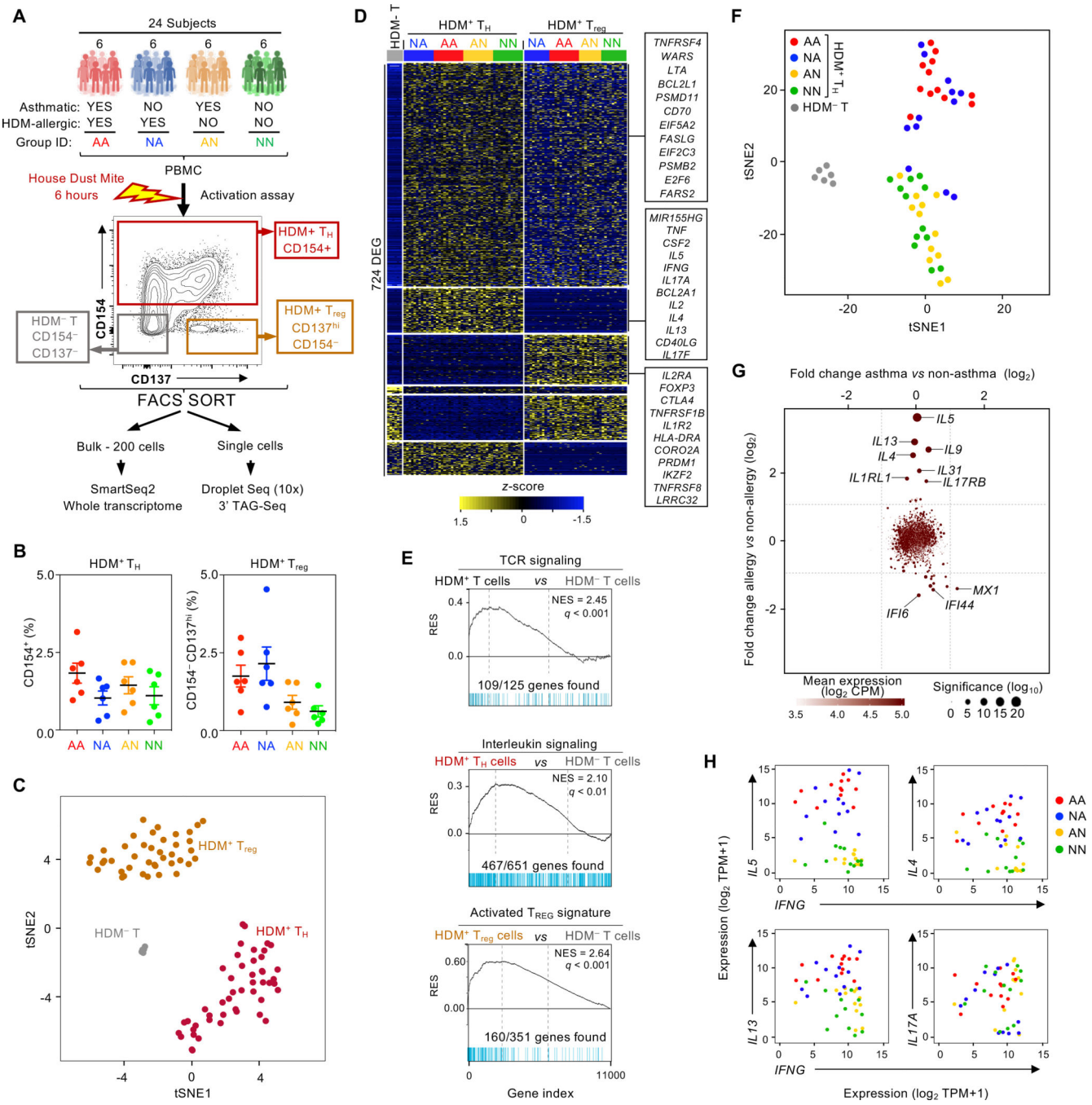

Fig. 1.

Bulk RNA-seq analysis of HDM allergen-reactive T cells does not identify asthma-specific features. (**A**) Schematic representation of the study summarizing the subject groups, activation assay, and sorting and sequencing strategies. (**B**) Dot plot showing the percentage of CD4 memory HDM-reactive T cells that were CD154^{+} (left) or CD154^{-} CD137^{+} (right) for each subject group. Horizontal line mean; error bar, standard error. (**C**) t-SNE plot of bulk RNA-seq samples: 6 HDM^{-} T cells (from asthma-allergic patients), 24 HDM^{+} T_H (from all patients), 18 HDM^{+} T_{reg} (from all patients)). (**D**) Heatmap of row-wise z-score-

normalized expression for 724 genes differentially expressed between the 3 groups of cells in Figure 1C. Each column represents data from one subject. (**E**) Gene set enrichment analysis (GSEA) of grouped bulk RNA-seq datasets presented in Figure 1C. q, false discovery rate; NES, normalized enrichment score; RES, relative enrichment score; list of genes provided in table S4. (**F**) t-SNE plot of bulk RNA-seq datasets for HDM^- T samples (N = 6) and T_H samples colored by disease group, where each dot represents one RNA-seq data from one subject (N = 12 per group). (**G**) Scatter plot shows log_2-fold change in expression of significantly differentially expressed genes between asthma (N = 24) versus non-asthma (N = 24) (x axis) and allergic (N = 24) versus non-allergic (N = 24) (y axis) T_H samples. (**H**) Scatter plots show co-expression of the indicated canonical T_H1 and T_H2 cytokines in T_H samples coded by disease group.

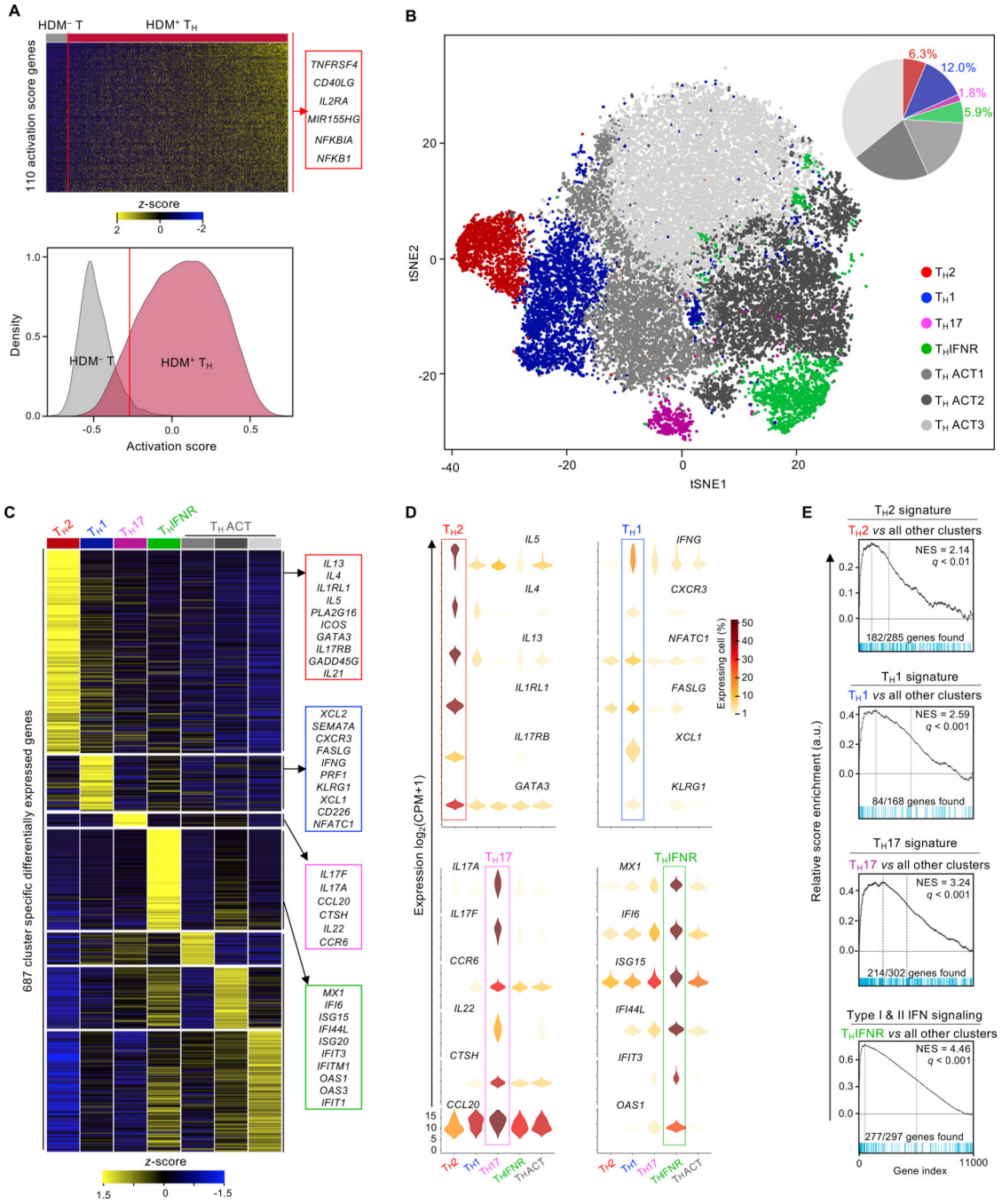

Fig. 2.

Single-cell RNA-seq clustering analysis reveals heterogeneity among HDM-reactive T_H cells. (**A**) Top - heatmap of row-wise z-score-normalized expression for 110 genes used to establish the activation score (see Methods), rows are ordered by hierarchical clustering. Each column represents a single-cell RNA-seq data, ordered by activation score. Right - examples of genes included in the T_H activation score. Bottom - histogram shows the density function of HDM^- T (N = 3,075, grey) and HDM^+ T_H (N = 31,105, red) cell activation scores (Methods). The red line indicates the threshold of selection (activation score of −0.27,

5 % of HDM^{-}). (**B**) t-SNE visualization of Seurat clustering analysis of approximately 28,313 single HDM^{+} T_H cell transcriptomes obtained from all 24 subjects. IFNR, interferon response; ACT, biologically uncharacterized activated T cells (3 groups). Top right - pie chart shows the cell number proportion of each cluster. (**C**) Heatmap of row-wise z-score-normalized mean expression of cluster-specific differentially expressed genes. Columns represent the average expression for each cluster, ordered based on biological relevance. Right - lists of biologically relevant example genes for each cluster. Equal numbers of cells were sampled from each cluster. (**D**) Violin plots show $\log_2$ (CPM+1) normalized expression in each cluster (3 T_HACT clusters merged) for 24 cluster-specific signature genes (6 per cell type). Color scale represents the fraction of cells within each cluster expressing the given gene, excluding cells with no expression. (**E**) GSEA between each cluster and other clusters of single-cell transcriptome datasets presented in Figure 2B. q, false discovery rate; NES, normalized enrichment score; RES, relative enrichment score; list of genes provided in table S4.

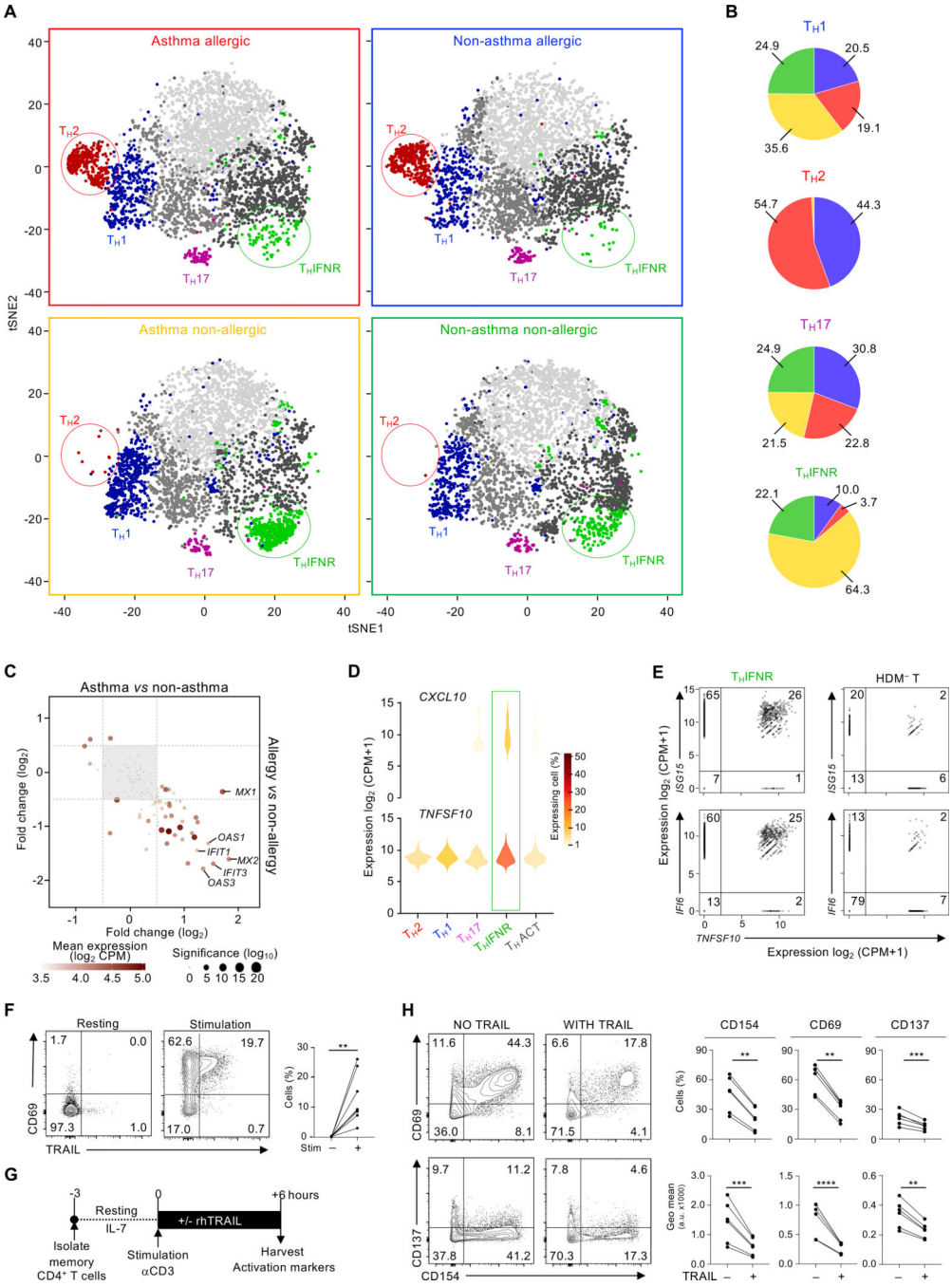

Fig. 3.

Proportions of HDM-reactive T_H subsets differ between allergic and non-allergic subjects. (**A**) t-SNE visualization of Seurat clustering analysis shown in Figure 2b, using equal cell numbers for each disease group (N = 3,720), obtained from all 6 subjects in each group. Cells are colored according to cluster as in Figure 2B. (**B**) Pie chart illustrating the relative proportion of cells from each disease group in the 4 biologically relevant clusters. (**C**) Scatter plot shows the log_2-fold change of expression of T_HIFNR signature genes between asthmatic (N = 12) versus non-asthmatic (N = 12) (x-axis) and allergic (N = 12) versus non-

allergic (N = 12) (y-axis) subjects among cells in the T_HIFNR cluster. Equal numbers of cells were sampled per group. Dotted lines indicate the threshold value of fold change for gene filtering. (**D**) Violin plots show $\log_2$(CPM+1) normalized expression of *CXCL10* and *TNFSF10* in each T_H cluster. Cells with no expression were excluded. (**E**) Scatter plots show co-expression of *TNFSF10* with the products of the T_HINFR signature genes *IFI6* and *ISG15* by T_HINFR cells (left) or HDM$^-$ T cells (right). Each dot represents one cell. (**F**) Contour plots show the expression of CD69 versus TRAIL in memory CD4$^+$ T cells before (left) and after 6 h (center) of TCR stimulation with anti-CD3 and anti-CD28. Both plots are representative of 5 independent experiments. Numbers indicate the percentage of cells in each quadrant. Right, quantification of each of the 6 experiments; bars represent the mean and standard error. (**G**) Diagram of the TRAIL functional assay. (**H**) Left, contour plots show the expression of the cell-activation markers CD154, CD69, and CD137 in memory CD4$^+$ cells after 6 h of stimulation in the presence or absence of TRAIL. Data shown are from a representative experiment. Right, quantification of each of the 6 experiments; bars represent the mean and standard error. *, $P < 0.1$; **, $P < 0.01$, *** $P < 0.001$.

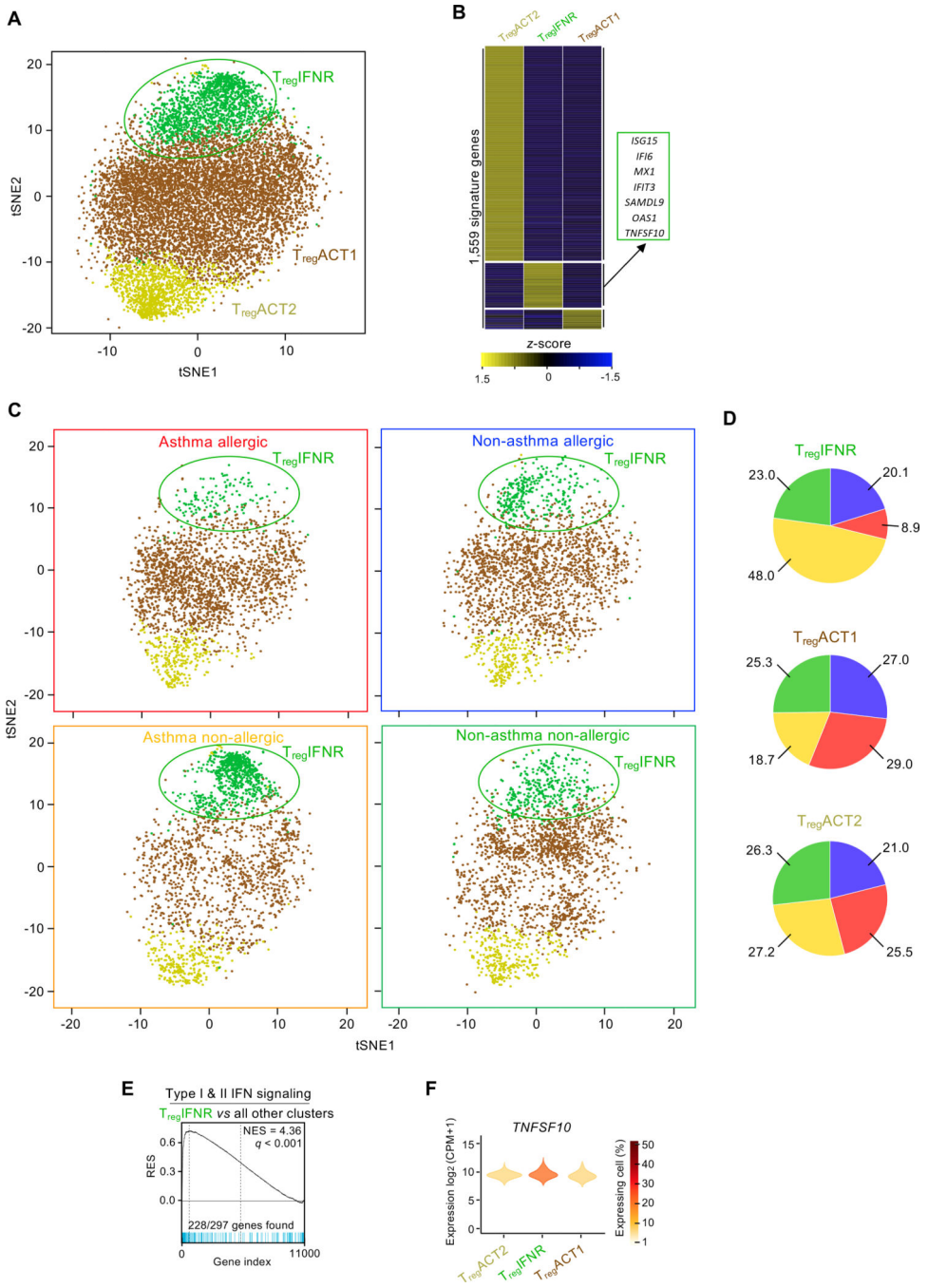

Fig. 4.

A subset of HDM-reactive T_{reg} cells express the interferon response signature. (**A**) t-SNE visualization of Seurat clustering analysis of the transcriptomes of 10,526 single HDM-activated T_{reg} cells obtained from all 24 subjects. (**B**) Heatmap showing hierarchical clustering of row-wise z-score-normalized mean expression of cluster-specific differentially expressed genes (N = 1,559) Columns represent each T_{reg} cluster. Right - lists of biologically relevant examples genes for the T_{reg}IFNR cluster. Equal numbers of cells were sampled per disease group. (**C**) t-SNE visualization of Seurat clustering analysis shown in

Figure 4A, using equal cell numbers for each subject group (n = 2,180) obtained from all 6 subjects. (**D**) Pie charts illustrate the relative proportion of cells from each subject group within each of the 3 T_{reg} clusters. (**E**) GSEA between each T_{reg}IFNR and the 2 other T_{reg} clusters. q, false discovery rate; NES, normalized enrichment score; RES, relative enrichment score; list of genes provided in table S4. (**F**) Violin plots show log_2(CPM+1) normalized expression of *TNFSF10* in each T_{reg} cluster. Cells with no expression are excluded (see Materials and Methods).

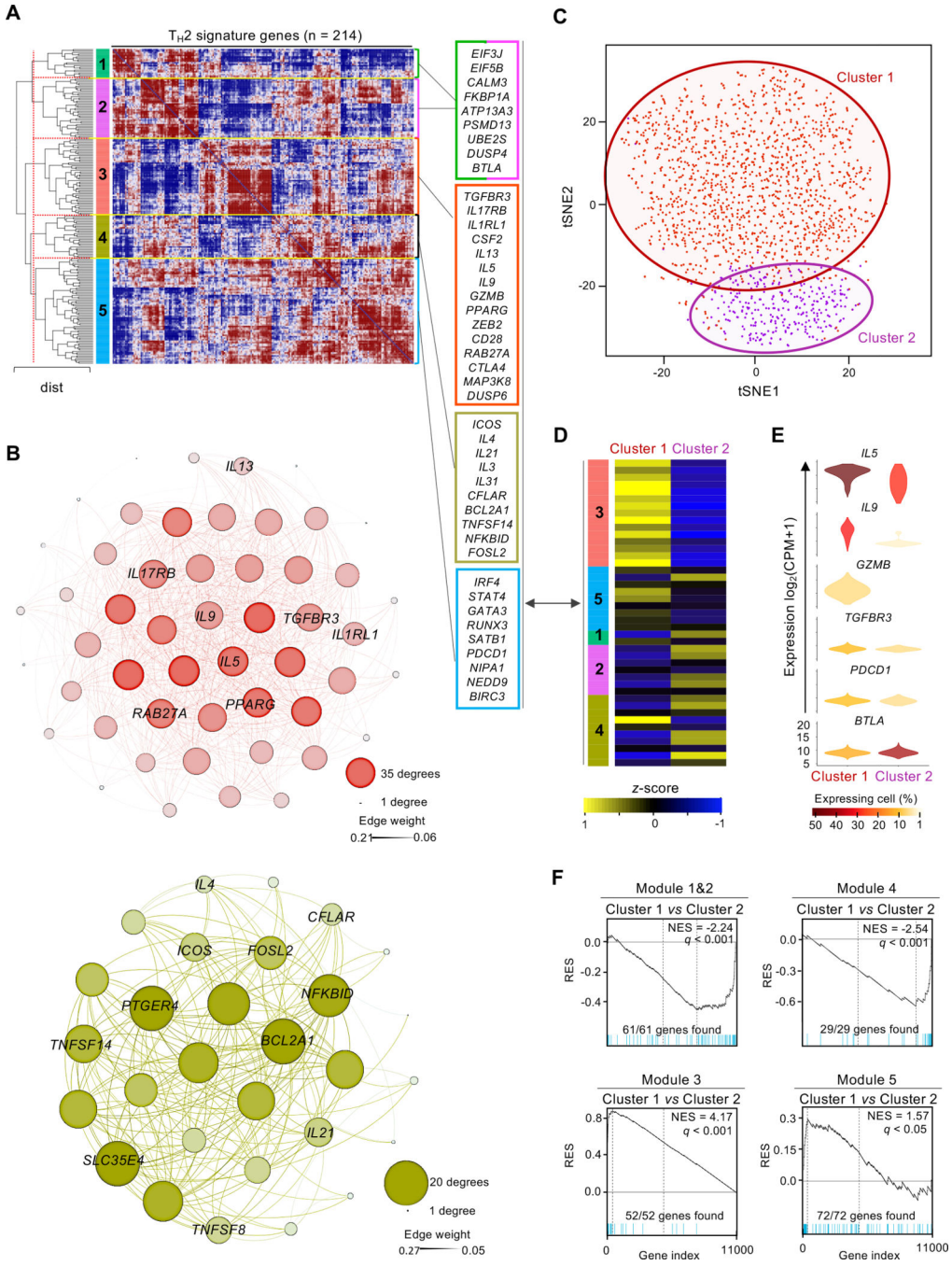

Fig. 5.

HDM-reactive T_H2 cells are enriched for transcripts linked to enhanced functionality. (**A**) Hierarchical clustering of Spearman correlation coefficient matrix for saver-imputed expression values of the 214 genes uniquely up-regulated in the T_H2 cluster. Values are clustered with complete linkage. Dotted red line indicates Euclidian distance threshold value used to define the 5 modules of co-expressed genes. Right – list of example genes for each module (modules 1 and 2 merged). (**B**) Gephi visualization of weighted correlation network analysis (WGCNA) for genes co-expressed in modules 3 (top) and module 4 (bottom) from

Figure 5A. Nodes correspond to a given gene and are sized based on the number of edges (connections); edges thickness correlates to strength degree of correlation. (**C**) t-SNE visualization of Seurat clustering analysis of single T_H2 cluster cell transcriptomes (N = 1,751) obtained from 12 allergic subjects regardless of asthma status (red, T_H2-cluster 1 (N = 1,440); purple, T_H2-cluster 2 (N = 311)). Red and purple circling lines represent limits of each T_H2 clusters 1 and 2, respectively. (**D**) Heatmap showing row-wise z-score-normalized mean expression of genes shown in Figure 5A between both T_H2 sub-clusters (columns). (**E**) Violin plots show $\log_2$(CPM+1) normalized expression for genes biologically relevant between both T_H2 sub-clusters. Color code represents the fraction of cells expressing the given gene in each T_H2 sub-cluster; cells with no expression are not included. (**F**) GSEA between T_H2 sub-clusters. Plots illustrate significative enrichment of module genes shown in Figure 5A between both T_H2 sub-clusters. q, false discovery rate; NES, normalized enrichment score; RES, relative enrichment score; list of genes provided in table S4.

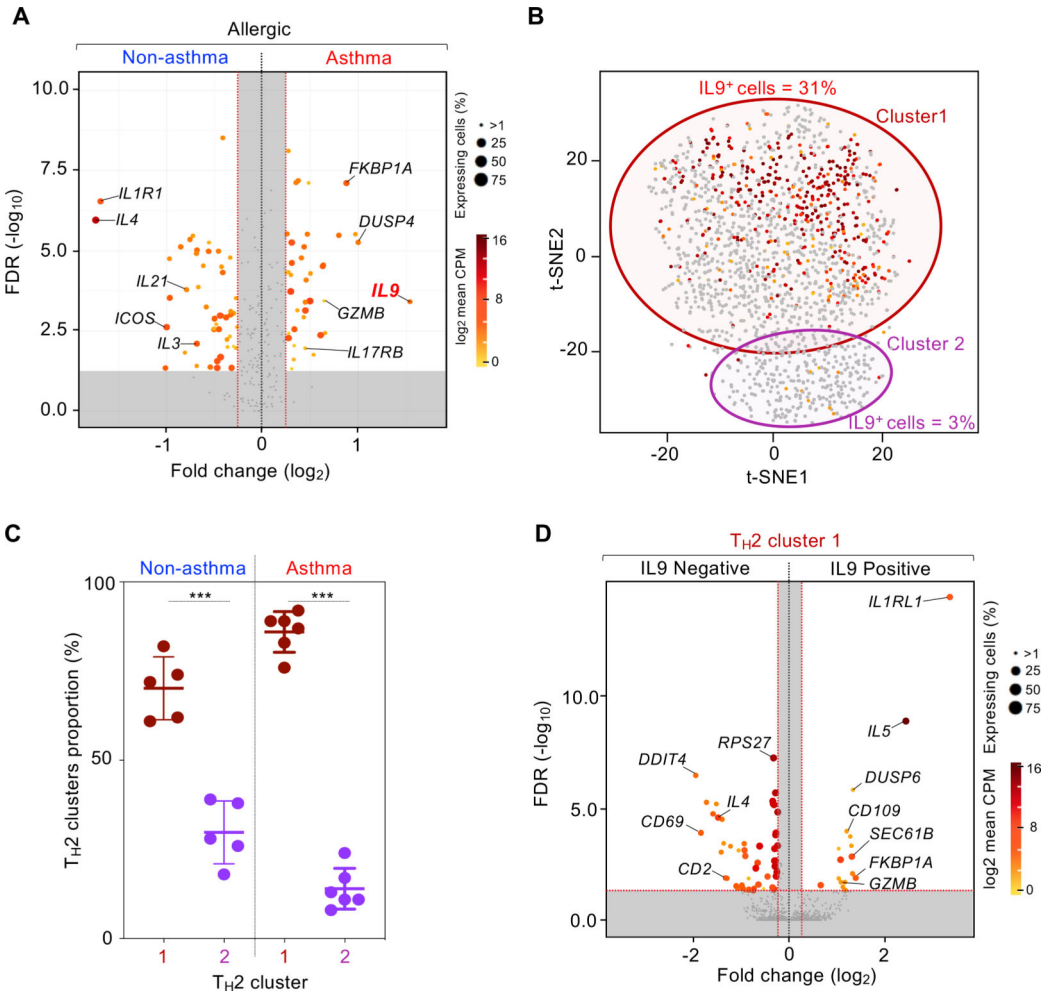

Fig. 6.

Asthma-specific T_H2 single cells analysis. (**A**) Volcano plot shows statistical significance (-$\log_{10}$ adjusted P-value) in function of the $\log_2$-fold difference in expression for filtered genes (see Materials and Methods), when comparing expression between T_H2 cells from asthma allergic (N = 6) versus non-asthma allergic (N = 6) subjects. Dots are colored accordingly to the average of expression ($\log_2$) and sized based on the fraction of cells expressing the given gene, both derived from the group in which the gene is upregulated. Equal numbers of cells where sampled in each group (N = 661). Grey dotted lines represent the threshold value for fold change (vertical, $\log_2(|FC|) > 0.5$-fold) and significance (horizontal, -$\log_{10}$(adjusted P-value) > 2). (**B**) t-SNE visualization of T_H2 cluster cell transcriptomes shown in Figure 5C in which each dot is a cell is cell colored according to expression for *IL9* (grey, none). Outlines represent T_H2 sub-cluster limits. (**C**) Box and whisker plot shows percentage of T_H2 cells in each sub-cluster in asthma allergic (N = 6) and non-asthma allergic (N = 5) subjects. Center line, median value; box, quartiles; whisker lines, 10^{th} and 90^{th} percentiles. **; P < 0.01. (**D**) Volcano plot similar to Figure 6A comparing expression between *IL9*-positive cells (N = 444) and I*L9*-negative cells (N = 444) in the asthma allergic T_H2 cluster 1.